Molecular Diagnosis & Therapy (2023) 27:193–226
https://doi.org/10.1007/s40291-022-00634-x

REVIEW ARTICLE

The Potential of Nanobodies for COVID-19 Diagnostics and Therapeutics

Dhaneshree Bestinee Naidoo[1] · **Anil Amichund Chuturgoon**[1]

Accepted: 5 December 2022 / Published online: 19 January 2023

Abstract

The infectious severe acute respiratory syndrome coronavirus-2 (SARS-CoV-2) is the causative agent for coronavirus disease 2019 (COVID-19). Globally, there have been millions of infections and fatalities. Unfortunately, the virus has been persistent and a contributing factor is the emergence of several variants. The urgency to combat COVID-19 led to the identification/development of various diagnosis (polymerase chain reaction and antigen tests) and treatment (repurposed drugs, convalescent plasma, antibodies and vaccines) options. These treatments may treat mild symptoms and decrease the risk of life-threatening disease. Although these options have been fairly beneficial, there are some challenges and limitations, such as cost of tests/drugs, specificity, large treatment dosages, intravenous administration, need for trained personal, lengthy production time, high manufacturing costs, and limited availability. Therefore, the development of more efficient COVID-19 diagnostic and therapeutic options are vital. Nanobodies (Nbs) are novel monomeric antigen-binding fragments derived from camelid antibodies. Advantages of Nbs include low immunogenicity, high specificity, stability and affinity. These characteristics allow for rapid Nb generation, inexpensive large-scale production, effective storage, and transportation, which is essential during pandemics. Additionally, the potential aerosolization and inhalation delivery of Nbs allows for targeted treatment delivery as well as patient self-administration. Therefore, Nbs are a viable option to target SARS-CoV-2 and overcome COVID-19. In this review we discuss (1) COVID-19; (2) SARS-CoV-2; (3) the present conventional COVID-19 diagnostics and therapeutics, including their challenges and limitations; (4) advantages of Nbs; and (5) the numerous Nbs generated against SARS-CoV-2 as well as their diagnostic and therapeutic potential.

Key Points

The advancement in current coronavirus disease 2019 (COVID-19) detection, diagnosis and treatments has had positive effects.

Advantages of nanobodies include rapid isolation, specificity, stability, fast large-scale production, aerosolization and affordability.

Nanobodies are a viable option for COVID-19 diagnostics and therapeutics.

✉ Anil Amichund Chuturgoon
chutur@ukzn.ac.za

[1] Discipline of Medical Biochemistry and Chemical Pathology, Faculty of Health Sciences, Howard College, University of Kwa-Zulu Natal, Durban 4013, South Africa

1 Introduction: Coronavirus Disease 2019 (COVID-19)

Coronaviruses are a part of the Coronaviridae family, and the first human coronaviruses (HCoV) were identified around the 1960s [1]. Coronavirus infections can be endemic (HCoV-229E, -OC43, -NL63 and -HKU1), which causes the common cold/mild illness, as well as epidemic (severe acute respiratory syndrome coronavirus [SARS-CoV], SARS-CoV-1, and Middle East respiratory syndrome coronavirus [MERS-CoV]), which may cause lethal respiratory infections [1]. These viruses emerge periodically and are associated with major outbreaks [2]. In November 2002, SARS-CoV-1 appeared and caused worldwide infection, with a 10% lethal rate [2, 3]. Thereafter, in June 2012, MERS-CoV emerged and showed a 35% lethal rate [2, 3].

More recently, in December 2019, severe acute respiratory syndrome coronavirus-2 (SARS-CoV-2) emerged in Wuhan, China [1, 3]. This highly contagious virus has swiftly spread throughout the globe, leading to coronavirus

disease 2019 (COVID-19) [4, 5] being declared a pandemic in March 2020 [3]. There have been more than 585 million COVID-19 cases and more than 6 million fatalities [6] worldwide [4, 5]. Virus transmission may occur through direct contact with infected individuals and exposure to SARS-CoV-2-contaminated liquid droplets, surfaces and materials [3]. Infected individuals may be asymptomatic (absence of all symptoms) or symptomatic (presence of symptoms) [7]. The common symptoms are fever (87%), cough (67%), shortness of breath, loss of taste, and fatigue (38%) [1, 3]. However, COVID-19 may worsen, resulting in pneumonia, multi-organ failure, and loss of life [1, 3].

The COVID-19 pandemic has resulted in many challenges to the human population, healthcare systems, and economic and social activities [8]. Notably, the global economic cost of the pandemic is over $10.3 trillion [9]. Initially, the world relied heavily on the implementation of protective/preventative measures as it is imperative to control virus transmission routes and infection sources [3]. These measures included decreased mass gatherings, use of protective gear (masks), effective sanitization, maintenance of personal hygiene, social distancing (2 meters), and a healthy diet/lifestyle (sufficient nutrition and vitamins) [3].

Population protective immunity or herd immunity refers to a high percentage of a population that is immune to a particular disease [7] with immunity being attained through infection or vaccination [7]. For COVID-19, approximately 67% of a population should be immunized to achieve herd immunity, which can potentially decrease the spread of disease [7]. Several SARS-CoV-2 vaccines have been developed, tested and administered in an attempt to reach population immunity, however the efficacy of vaccines are negatively affected by the emergence of various strains [7].

Currently, several COVID-19 treatment options are available [1, 3]. Drug repurposing and *in vitro* inhibition have determined drugs that can be used [1], and some drugs/antibodies (Abs) have been approved by the US FDA for COVID-19 emergency treatment [1]. However there are limitations and challenges with conventional COVID-19 diagnosis and treatment options. Therefore, great strides continue to be made in the development of effective preventative, diagnostic and therapeutic agents to combat COVID-19.

2 Severe Acute Respiratory Syndrome Coronavirus-2 (SARS-CoV-2)

The SARS-CoV-2 genome comprises of open reading frames (ORFs) that encode various proteins [3]. At the 5′-terminal region, non-structural proteins (NSPs) essential for virus replication are encoded by ORF1 and ORF2, whereas the 3′-terminal region encodes functional structural proteins (spike [S], envelope [E], membrane [M], nucleocapsid [N] and 8 accessory proteins) [3]. The M, E and S proteins are located in the viral envelope, whereas the N protein is found in the core of the virus (Fig. 1) [2]. These proteins have specific and vital roles that allow the virus to survive and thrive in host cells (Fig. 1) [2].

The ectoenzyme angiotensin-converting enzyme 2 (ACE2) is situated on the cell plasma membrane in various organ tissues but is widely distributed on epithelial cells of the respiratory tract [2, 3]. The ACE2 receptor is utilized by SARS-CoV-2 to enter human cells [3]. The S protein contains the receptor binding domain (RBD) and binds with high affinity to the ACE2 receptor by forming a transmembrane homotrimer [3]. It has two subunits, S1 and S2, that function in ACE2 binding and viral fusion to cell membranes, respectively [3]. Additionally, S protein priming is required for entry into cells [10]. Cellular proteases (TMPRSS2 or cathepsin) prime the S protein by cleavage, which leads to viral and cellular membrane fusion [10]. The

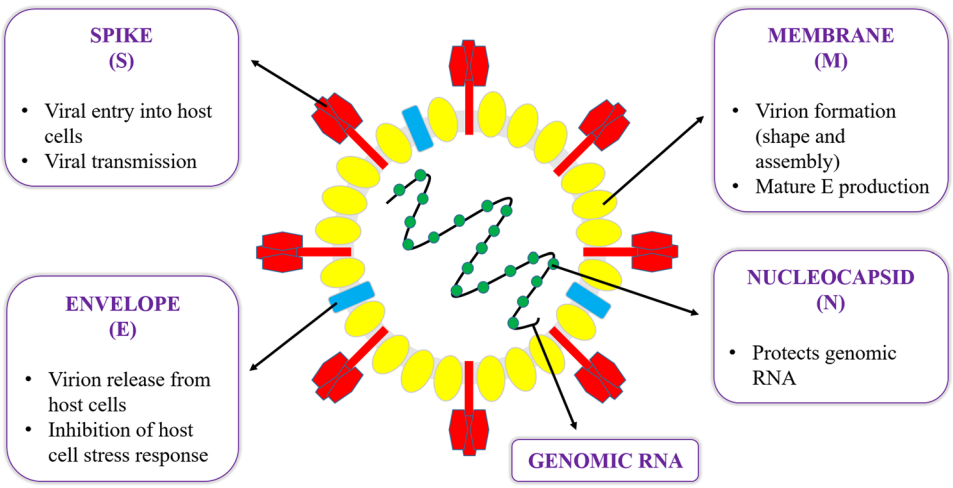

Fig. 1 General structure of SARS-CoV-2 and function of structural proteins. *SARS-CoV-2* severe acute respiratory syndrome coronavirus-2

RBD can be in an up-state (accessible/active) or down-state [11] (inaccessible/ inactive). The accessible conformation has at least one RBD in an up-state, whereas the inaccessible conformation has all the RBDs in a down-state. The S protein oscillates between the active and inactive conformation [11]. Notably, the RBD in the accessible up-state is needed for ACE2 to bind and allow cleavage by cellular proteases, resulting in a conformational change in S2 which allows viral entry [11]. Therefore, neutralizing agents may bind to the RBD-up conformation, thus inhibiting infection, or bind to the RBD-down conformation, which ultimately prevents viral entry [12].

After viral entry, SARS-CoV-2 proceeds to release its genetic material, which is translated into viral replicase polyproteins (pp) [2, 3]. These proteins are cleaved by viral proteinases, leading to the formation of functional NSPs (helicase [Hel] and the RNA-dependent RNA polymerase [RdRp]) that are responsible for structural protein RNA replication [3]. Notably, the S protein, ACE2 and TMPRSS2 are promising drug targets [10].

The emergence of variants (Table 1) such as Alpha (B.1.1.7, UK), Beta (B.1.351, South Africa [SA]), Gamma (P.1, Brazil), Delta (B.1.617.2, India) and Omicron (B.1.1.529, Botswana/SA) [13] are of great concern [14, 15]. Each of these variants lead to a new wave of infections and can potentially evade host immunity (developed post infection or vaccination) as well as therapeutics [14, 15]. Notably, the Omicron variant has been shown to be more transmissible, have an increased rate of infections, higher re-infection risk profile, greater immune escape capabilities and the largest number of mutations compared with the other variants (Table 1) [6, 13, 15]. Notably, individuals infected with the Delta and Beta variant have a 40% and 60% chance of re-infection with the Omicron variant, respectively [13]. Mutations in the S protein, such as E484K and N501Y, have been identified in the Brazil, SA, and UK variants (Table 1) [16]. Mutations such as D614G, N501Y, and K417N allow the virus to be more infectious, while the H655Y, N679K, and P681H mutations allow the virus to be more transmissible [6]. These mutations alter RBD epitopes, allow the virus to escape Ab neutralization, evade host immune responses, may render treatments ineffective [4], and enhance receptor binding specificity, virus growth [16], infectivity and virulence [17].

Notably, SARS-CoV-2 strains have been associated with devastating outbreaks, greatly increased infection rates and decreased vaccine efficacy [4]. Additionally, the continuous emergence of new variants has the potential to cause waves of infection in populations that already achieved protective immunity against previous strains [4]. Taken together, variants and associated mutations may negatively impact Ab and vaccine efficacy, which increases the number of Abs and vaccines required for protective and therapeutic purposes [16].

3 Current Diagnosis Methods for COVID-19

After the SARS-CoV-2 outbreak, diagnostic tests were rapidly developed in order to detect the virus earlier rather than later [3]. Specimen collection by nasopharyngeal swabs are preferred and accepted for molecular analysis/detection [3,

Table 1 SARS-CoV-2 variants of concern, and their mutations [4, 6, 18, 19]

Emergence country and date	SARS-CoV-2 variant	Mutations
UK September 2020	B.1.1.7/Alpha	H69del, V70del, Y144del, N501Y, A570D, D614G, P681H, T716I, S982A, D1118H, D3L, R203K, G204R, S235F, T1001I, A1708D, I2230T, S3675del, G3676del, F3677del, P314L, Q27*, R52I, Y73C
South Africa May 2020	B.1.351/Beta	D80A, D215G, L241del, L242del, A243del, K417N, E484K, N501Y, D614G, A701V, T205I, P71L, T265I, K1655N, K3353R, S3675del, G3676del, F3677del, P314L, Q57H
Brazil November 2020	P.1/Gamma	L18F, T20N, P26S, D138Y, R190S, K417T, E484K, N501Y, D614G, H655Y, T1027I, V1176F, P80R, R203K, G204R, S1188L, K1795Q, S3675del, G3676del, F3677del, P314L, E1264D, S253P, E92
India October 2020	B.1.617.2/Delta	T19R, E156del, F157del, R158G, L452R, T478K, D614G, P681R, D950N, D63G, R203M, D377Y, I82T, P314L, G662S, P1000L, S26L, ORF7a V82A, T120I, ORF8 Q27*, R52I, Y73C, E92K D119del, F120del, ORF9b T60A
South Africa November 2021	B.1.1.529/Omicron	A67V, H69del, V70del, T95I, G142del, V143del, Y144del, Y145D, N211del, L212I, G339D, S371L, S373P, S375F, K417N, N440K, G446S, S477N, T478K, E484A, Q493R, G496S, Q498R, N501Y, Y505H, T547K, D614G, H655Y, N679K, P681H, N764K, D796Y, N856K, Q954H, N969K, L981F, P13L, E31del, R32del, S33del, R203K, G204R, T9I, D3G, Q19E, A63T, K856R, S2083del, L2084I, A2710T, T3255I, P3395H, L3674del, S3675del, G3676del, I3758V, P314L, I1566V, P10S, E27del, N28del, A29del

SARS-CoV-2 severe acute respiratory syndrome coronavirus-2

20]. However, in the absence of nasopharyngeal swabs, nasal secretions, blood, sputum, and bronchoalveolar lavage samples are collected [3, 21]. Notably, viral RNA load, which can affect detection methods, is usually highest between 0 and 4 days (89%) and then decreases between 10 and 14 days (54%) [20]. Unfortunately, sample collection can be uncomfortable for the patient and sample processing is a lengthy procedure requiring a laboratory facility. Additionally, both sample collection and processing require trained personal. Specimens are evaluated using virus-specific serological and molecular tests in order to provide a diagnosis [21]. Specific SARS-CoV-2 proteins are identified using enzyme-linked immunosorbent assay (ELISA), antigen tests, point-of-care (POC) blood test or Western blots (serological tests), while specific SARS-CoV-2 genes are detected using quantitative polymerase chain reaction (qPCR), real-time PCR (RT-PCR) or northern blot hybridization (molecular tests) [7, 20–22]. Initially, positive cases were identified using RT-PCR; thereafter, ELISA kits and various other tests were developed [3].

The RT-PCR technique is an accurate assay regularly utilized for SARS-CoV-2 detection and diagnosis [8, 22]. Currently, there are various COVID-19 RT-PCR kits commercially available that target various viral genes (RdRp, E, N, S, ORF1ab, ORF1a, and ORF1b or ORF8) for detection [8, 20, 23]. Notably, RT-PCR has been considered the gold standard but there are advantages and challenges. RT-qPCR provides reliability, flexibility, high sensitivity and specificity, however the challenges include false negatives, a lengthy and complex procedure, requirement of expensive equipment and trained personnel, sample quantities for RNA isolation, sample integrity, low viral load samples, and delivery time of results to patients (> 24 h) [23, 24]. Additionally, mutations in the target regions have the potential to effect RT-PCR accuracy, resulting in test failures and false-negatives [20]. However, researchers are developing specific primers to allow the detection of major variants [20].

The Omicron variant can affect RT-PCR test performance, e.g. the Thermo Fischer TaqPath assay attributable to the 69–70 deletion [25], which can lead to the failure of certain PCR assays [13]. This indicates the importance of tests targeting more than one genomic region of SARS-CoV-2, as this may prevent test failures and false negative results [25]. Notably, PCR diagnostics can determine the SARS-CoV-2 cases that need sequencing to detect Omicron cases [13]. In the Alpha variant S gene, amino acids 69 and 70 are deleted (Δ69–70), resulting in the absent/negative S-gene (S−), whereas the Delta variant does not contain the 69–70 deletion, resulting in a positive S-gene (S+) [13]. The Omicron variant S-gene also contains the 69–70 deletion [13]. Since the Alpha variant cases have decreased considerably, the S− results (suspect Omicron infection) could be used as a marker, together with sequencing, for Omicron detection [13, 25]. However, variants do have sub-lineages and the Omicron BA.2 sub-lineage does not contain the 69–70 deletion, hence it is S+ [6]. Therefore, whole-genome sequencing with next-generation sequencing is required for confirmation of the Omicron variant even though it is a lengthy and expensive process [6, 26].

Loop-mediated isothermal amplification (LAMP) has been considered a reliable alternative to conventional RT-PCR [20]. It is a fast and cheap method that is highly specific due to the use of 6–8 specific primer sequences that detect eight different regions [20]. Additionally, it can identify SARS-CoV-2 from swabs or saliva without the requirement of RNA isolation [23]. The RT-LAMP method is inexpensive, fast, and highly specific, however sensitivity is dependent on viral load [24]. Notably, proper primer design and use of specific primers are essential to maximize sensitivity [23].

The ELISA method is a cost-effective quantitative, qualitative, highly specific, sensitive, efficient and simple procedure [23]. ELISAs are reliable, commercially available kits that mostly detect the S and N proteins [20]. However, the ELISA success rate is greatly dependent on the stage of COVID-19 and the viral load [20]. Additionally, ELISAs can detect Abs produced against a specific viral antigen (S and N proteins) [20]. Several kits measure the ratio between immunoglobulin (Ig) M and IgG [20]. ELISA sensitivity and specificity were shown to be 85.7–80% and 98.5–100%, respectively [24]. ELISAs are able to detect recent or previous SARS-CoV-2 exposure, however challenges include sample quantity, sample integrity and lengthy assay procedure, and results are dependent on a patient's immunity (IgG and IgM) and delivery time of the results (> 24 h) [24].

Lateral flow assays (LFAs) identify SARS-CoV-2 antigens (N) and anti-SARS-CoV-2 Abs (IgG and IgM) [24]. It is a simple, qualitative test that does not require specialized/expensive laboratory equipment [24]. LFAs are used as POC testing and are small in size, fast, sensitive (90%), specific (98%), stable, and low in cost [23]. However, LFAs can produce false-negative results due to low viral load samples [24]. Mistry et al. reviewed the literature on LFAs in order to assess sensitivity and specificity [27]. The percentage sensitivity of assays showed a wide range of 37–99%, whereas specificity was 92–100% [27]. The CORIS and BIOSENSOR assays were the lowest in sensitivity (45%), whereas the most evaluated Panbio Abbott assay had a sensitivity of 78.41% [27]. The specificity of all assays was > 93% [27]. Notably, the BD Veritor, BIOCREDIT, COVID-VIRO assays showed 100% specificity [27].

Antigen-detecting diagnostic tests allow for rapid and inexpensive delivery of results [28]. Commercially available tests include the Panbio (Abbott), Standard Q (SD Biosensor/Roche), Sure Status (Premier Medical Corporation), 2019-nCoV (Wondfo), Beijng Tigsun Diagnostics Co. Ltd. (Tigsun), Onsite (CTK Biotech), Acon Biotech (Flowflex), and the NowCheck Covid-19 Ag test (Bionote) [28].

Notably, five of these tests (Panbio, SD Biosensor, Sure Status, Onsite, and Acon) are on the World Health Organization (WHO) emergency use listing [28]. Bekliz et al. investigated the sensitivity of these eight tests against the variants [28]. Compared with other variants, these tests showed a general lower sensitivity to Omicron BA.1 in cultured virus and in infectious virus analysis [28]. Notably, the Acon test demonstrated the most sensitivity for Omicron-BA.1 and most other variants [28].

Hardick et al. compared the sensitivity of POC antigen assays (BD Veritor, Abbott BinaxNow, Orasure InteliSwab and Quidel QuickVue) in detecting the Omicron and Delta variants [29]. Results showed that the assays with the highest sensitivity for the Omicron variant were Abbott BinaxNow and Orasure InteliSwab, whereas those with the highest sensitivity for the Delta variant were Orasure InteliSwab and Quidel QuickVue [29]. Notably, only the QuickVue assay detected all SARS-CoV-2 RT-PCR-positive nasal/nasopharyngeal swab samples [29]. The Omicron variant was identified by these rapid antigen tests, however there is still a decreased sensitivity of antigen tests compared with molecular tests [29]. At high virus levels, the BinaxNOW test (Abbott) was shown to identify infections with variants, including the Omicron variant [30]. However, at low virus levels (early stage of infection), the BinaxNOW test may indicate a negative result, thus a confirmatory RT-PCR should be conducted [30].

Antigen detection tests that target the N antigen can prevent test invalidation due to changes in the S protein [25]. However, the Omicron variant has some mutations in its N sequence which may negatively impact the N antigen detection tests [25]. In comparison with PCR tests, some studies have indicated that about half of the positive cases identified by rapid tests are false positives [6]. Generally, antigen tests have been less sensitive than RT-PCR tests, therefore negative antigen test results should be verified by an RT-PCR test, especially for a possible Omicron infection [6, 25]. There are also mutation-specific tests (E484K/Q, L452R, N501Y) that identify mutations that can be linked to the variants [25].

Clustered regularly interspaced short palindromic repeats (CRISPR) have the potential to provide rapid, accurate and portable diagnostic assays [20, 31]. The principle of the technology is that CRISPR RNA (crRNA) can bind to specific target sequences and activate CRISPR and CRISPR-associated (Cas) enzymes such as Cas9, Cas12, and Cas13 [23, 31]. This has been referred to as next-generation diagnostics, and CRISPR-Cas technology has been utilized in the development of tools to identify SARS-CoV-2 infection [31]. Liang et al. (2021) developed and validated a CRISPR-Cas12a-based multiplex allele-specific assay for SARS-CoV-2 variant identification that is highly sensitive and specific [31]. The assay is capable of identifying single nucleotide mutations and recognizing variants (Alpha, Beta and Delta) based on a combination of various crRNAs that are specific for vital SARS-CoV-2 mutations (K417N, L452R/Q, T478K, E484K/Q, and N501Y) [31]. Notably, it requires a comprehensive interpretation of multiple results due to no single mutation, or one crRNA could distinguish between all variants [31]. Thereafter, Liang et al. investigated the use of the CRISPR-Cas12a assay for detection of the omicron variant [32], and the results indicated that one crRNA containing 3–4 mutations was able to identify and diagnose the variant [32]. Finally, the CRISPR-Cas12a assay was shown to detect major variants of concern (Alpha, Beta, Delta, and Omicron) in clinical samples [33]. Wang et al. described the detection method, light-up CRISPR-Cas13 transcription amplification, which can target and identify SARS-CoV-2 as well as mutated variants [34]. The ligation process and Cas13a/crRNA recognition ensures sequence specificity (detects mutations), while the light-up RNA aptamer leads to the sensitive output of signals [34]. This assay may be useful in detecting SARS-CoV-2 in swabs and food packages [34]. The CRISPR method is fast and simple and expensive equipment is not needed, however virus mutations can cause false results [24].

Diagnostic and treatment interventions should target conserved areas due to the development of mutations in certain areas [26]. Therefore, the current research is focused on developing SARS-CoV-2 detection assays that are cost effective, have easy sample collection (e.g. saliva or finger prick), are user friendly (conducted by the patient), and have rapid indication of results (15–30 min).

4 Current Treatments for COVID-19

The pandemic lead to an urgent need for treatments to combat the disease and save lives. Treatments that disrupt the lifecycle may decrease viral replication and spread, whereas treatments that target host receptor proteins can decease/block virus attachment and entry [35]. Various treatment options have been proposed for SARS-CoV-2, such as repurposing of antiviral treatments, passive immunotherapy, vaccines and Abs. Although these options have been beneficial to a certain extent, there have been various limitations and challenges observed with their use.

4.1 Antiviral Treatments

Repurposed antiviral treatments have been investigated for their possible use and are under investigation in randomized controlled trials (RCTs) [3]. The drugs included lopinavir (LPV), ribavirin, favipiravir (FPV), remdesivir, chloroquine, molnupiravir, nirmatrelvir, and paxlovid.

Previously, *in vitro* and *in vivo* studies demonstrated that LPV (antiretroviral protease inhibitor) [36] impeded coronavirus protease activity [3]. Furthermore, the LPV and ritonavir (RTV; inhibits LPV metabolism) combination treatment has been used for SARS-CoV-1 and MERS-CoV [3]. However, in severely SARS-CoV-2 infected individuals, the LPV/RTV treatment demonstrated no benefit [3, 37]. Şimşek-Yavuz et al. reviewed and analyzed data from randomized clinical trials and concluded LPV/RTV was ineffective and should not be utilized [38]. Moreover, a systematic review of RCTs reported that in COVID-19 patients, LPV/RTV utilization did not provide any significant clinical improvement and adverse reactions were notable [39].

The guanosine nucleoside analog ribavirin depletes intracellular guanosine, increases interferon (IFN) gene expression, and targets viral RdRp [3, 36]. In a MERS-CoV study, ribavirin and IFNα-2b treatment was promising [36]. However in respiratory patients, ribavirin decreases hemoglobin concentrations, which decreases its antiviral potential against SARS-CoV-2 [36]. FPV is also a guanosine analog that targets RdRP [36]. In COVID-19 patients, FPV improved fever and cough but did not improve the recovery rate [40]. Qomara et al. reviewed RCTs of antiviral drugs and the results indicated that the clinical status of patients was improved following FPV treatment, but there was no significant change in clinical recovery [39].

Remdesivir (an adenosine nucleotide analog) has shown antiviral activity against SARS-CoV-1 and MERS-CoV [3, 36]. It inhibits RdRp, integrates into viral RNA, and decreases viral RNA production [20, 36]. Remdesivir has also been shown to inhibit SARS-CoV-2 proliferation (*in vitro*) [36, 41]. The FDA approved remdesivir for COVID-19 treatment in adult, pediatric and old-age patients [6]. In a COVID-19 clinical trial, remdesivir treatment demonstrated clinical improvement (68%) in individuals [42], but it should not be used in patients receiving invasive ventilation due to increased mortality rates noted [42]. A review of RCTs revealed that the potential benefits of remdesivir treatment in hospitalized patients included faster recovery time, decreased length of hospitalization, and respiratory adverse effects, but its effect on decreasing mortality was unclear [39].

Chloroquine increases endosomal pH, interferes with M protein proteolytic processing, alters virion assembly, and interferes with ACE2 receptor and S protein glycosylation, ultimately blocking viral infection [3, 36]. It was shown to inhibit SARS-CoV-2 *in vitro* [36]. During SARS-CoV-2 infection, an increase in interleukin (IL)-6 and IL-10 levels was noted [3]. Chloroquine and hydroxychloroquine (chloroquine derivative) have demonstrated immunomodulatory effects as well as the capability of suppressing IL-6 and IL-10 immune responses [3]. The adverse effects of hydroxychloroquine and chloroquine treatment may be severe, e.g. cardiac arrhythmia [43]. Notably, a chloroquine overdose is toxic and fatal [36]. Initially, clinical studies demonstrated the potential of chloroquine/hydroxychloroquine as an effective COVID-19 treatment [44], and more recently, Axfors et al. estimated the effects of hydroxychloroquine and chloroquine by reviewing and analyzing data from RCTs [43]. Their results concluded that chloroquine treatment produced no benefit, whereas hydroxychloroquine treatment was associated with increased COVID-19 patient mortality [43]. Additionally, Şimşek-Yavuz et al. concluded that hydroxychloroquine was ineffective and should not be utilized [38].

Molnupiravir targets viral RNA polymerase and integrates into SARS-CoV-2 genetic information, leading to a change in the virus [6] and ultimately inhibiting/preventing further replication [45]. The FDA approved molnupiravir for emergency use for COVID-19. Molnupiravir and nirmatrelvir have been shown to inhibit viral polymerase and protease (e.g. 3CL protease) [6], resulting in a decrease in disease progression [45]. Utilization of a molnupiravir and nirmatrelvir combination has a great antiviral effect [26] and has demonstrated efficacy against Omicron infection [26, 46].

Paxlovid interferes with the SARS-CoV-2 processing proteins, which prevents transmission [26, 46], and has shown potential against COVID-19 [26]. The FDA approved paxlovid (nirmatrelvir tablets and RTV tablets) for emergency use in COVID-19 patients experiencing mild to moderate symptoms and who were at high risk of developing severe illness [6].

Notably, molnupiravir, nirmatrelvir, remdesivir, and paxlovid have demonstrated neutralizing activity against variants, including Omicron [6, 45]. Lai et al. reviewed and analyzed data from RCTs to determine the clinical efficacy and safety of antiviral drugs for non-hospitalized COVID-19 patients [47]. Their results indicated that antiviral drugs were related to a significantly lower risk of hospitalization/death [47]. Additionally, nirmatrelvir plus RTV was the best antiviral treatment with the lowest hospitalization/death risk, followed by remdesivir and molnupiravir [47].

Antiviral therapy that rapidly decreases viral load may improve patient outcomes and limit virus transmission [26].

Antiviral drugs have been approved and have shown some potential against COVID-19, however some may have lower SARS-CoV-2 specificity especially due to mutations/variants [48]. In COVID-19 patients, antiviral drugs have been prescribed and accepted but further research is needed to determine and understand the potential negative effects [26]. Thus, the continual development of therapeutics is essential.

4.2 Vaccines

Vaccines are a preventative option [7] and SARS-CoV-2 vaccine categories include mRNA, adenoviral vector, and inactivated and recombinant subunit vaccines [49]. There are approximately 216 COVID-19 vaccines in development and 92 are in human clinical trials [49]. The WHO has approved certain vaccines for emergency use, such as the BNT162b2

(Pfizer-BioNTech) and mRNA-1273 (Moderna Biotech) mRNA vaccines, the ChAdOx1 (AZD1222) (AstraZeneca) and Ad26.COV2.S (Janssen/Johnson & Johnson) adenoviral vector vaccines, the Coronavac (Sinovac Life Sciences) and COVAXIN (Bharat Biotech) inactivated vaccines, and the Nuvaxovid (Novavax) and Covovax (Serum Institute of India) recombinant subunit vaccines [49].

To date, a number of SARS-CoV-2 vaccines have been administered to the population and have proven to be effective to a certain degree [13]. The rAd26-S and rAd5-S adenoviral vector vaccines are well tolerated, induce strong immune responses, and stimulated similar concentrations of neutralizing Abs as recovered COVID-19 patients [50]. Jackson et al. revealed that the mRNA-1273 vaccine stimulated immune responses against SARS-CoV-2 [51]. Notably, the Pfizer vaccine successfully prevented COVID-19 by approximately 90% [7], and its efficacy against hospitalization was about 93% [45].

However, there have been recurring SARS-CoV-2 infections, which suggests that certain individuals do not develop a highly protective immune response and do not sufficiently respond to vaccinations [4]. Additionally, studies have shown that 6 months after vaccination, the level of serum neutralizing Abs greatly decreased [15]. To make matters worse, several highly virulent and transmissible strains have been identified, which affects the efficacy of current vaccines and treatments [4]. Notably, in individuals who have recovered from a COVID-19 infection or received an mRNA vaccine (two doses), the poly-mutant S was mostly fully resistant to neutralizing Abs [13].

Previously, most vaccines have shown effectiveness against the Alpha variant, however vaccine efficacy was considerably reduced against the Beta variant and further reduced against the Gamma variant [49]. For example, in individuals who received the CoronaVac vaccine, the neutralizing Abs against the variants were decreased by 2.9- 12.5-fold (Alpha, 2.9-fold; Beta, Gamma, Delta, and Omicron, 12.5-fold) [52]. The BNT162b2 vaccine-induced Ab titers decreased by 4- to 6-fold for Delta compared with the Alpha variant [53]. The efficacy of the AZD1222 and BNT162b2 complete vaccinations was 67–88 % against the Delta variant compared with 74–94% for the Alpha variant [53].

The Omicron variant showed a greater resistance against vaccine-induced immunity [53]. In SA, vaccine efficacy against infection decreased by the Delta and Omicron variants by 80% and 33%, respectively [13]. Furthermore, vaccine-induced (mRNA-1273, Sputnik, Sinopharm, Ad26.COV2.S, BNT162b2, AZD1222) neutralizing Ab titers against the Omicron variant significantly decreased [53]. For instance, Ab titers induced by BNT162b2 and AZD1222 against Omicron were 36- to 44-fold lower (*in vitro*) [53]. In comparison with the original strain, both the mRNA1273 and AstraZeneca complete vaccinations showed a decrease in neutralizing Abs against the Omicron variant by 74-fold and 14- to 21-fold, respectively [45]. Although, COVID-19 vaccines based on wild-type demonstrated reduced efficacy against the variants, they are still effective against the development of severe disease, hospitalization, and death [13, 15]. For example, the efficacy of the Pfizer-BioNTech vaccine is decreased by the Omicron variant but still decreases the risk of hospitalization (70%) [13].

Due to the continuous emergence of several SARS-CoV-2 variants, there is a requirement for booster vaccines or new vaccines that are tailored against various strains. Previous studies have demonstrated that heterologous boosters have greater neutralization efficacy against variants than the homologous vaccines [26, 49, 53]. Notably, a booster vaccination is able to restore Ab levels, enhance vaccine efficacy and provide protection against variants, including Omicron [13, 15, 54]. In polyclonal sera from BNT162b2 (two doses) vaccinated and recovered individuals, there was a lack of neutralizing activity against the Omicron variant as well as resistance to monoclonal Abs (mAbs) [55]. Notably, mRNA booster immunizations led to a marked increase in neutralizing activity against the Omicron variant in these individuals [55]. An mRNA booster vaccine was shown to induce strong variant cross-neutralization [45]. In comparison with the Wuhan strain, post mRNA vaccine BNT162b2 (two doses) showed a > 22-fold decrease in Omicron-neutralizing Ab titers; however, after a booster dose, the levels were increased 23-fold [56]. In individuals vaccinated with adenovirus or inactivated vaccines, an mRNA vaccine booster can induce elevated levels of neutralizing Abs against the Omicron variant [49].

Previously, a vaccine targeting the mutant S demonstrated that the level of neutralizing Abs against mutant viruses was high, but Ab levels against wild-type were lower [15, 57]. Although booster vaccines increase neutralizing activity against the Omicron variant, the neutralizing activity is still lower than the neutralizing activity against the original strain [45]. Polyvalent vaccines elicit Abs against diverse epitopes and are therefore able to be effective against several variants [26]. Taken together, continuous research is vital to develop bivalent vaccines (targeting wild-type and variants) and variant-specific vaccines (against the Omicron variant) [15, 57].

4.3 Passive Immunotherapy and Antibodies

Therapeutic options for COVID-19 may include passive Ab therapy that can reduce virus replication and disease severity [35]. Passive immunotherapy utilizes Abs that recognize epitopic regions in a virus [35]. These Abs can be isolated from infected individuals and/or scientifically produced in a laboratory [35].

A form of immunotherapy is early convalescent plasma (CP) or hyperimmune Ig administration [35]. Infected individuals develop a specific immune response/Abs against SARS-CoV-2, therefore the CP can be obtained from

recovered patients who have significant Ab titers [7, 35]. This therapy may be effective in virus neutralization, prevention of future infection, reduction in viral load, and mortality [7, 35]. The FDA authorized high-titer CP treatment for emergency use in hospitalized patients with compromised humoral immunity and/or early-stage disease [9]. Data from 16 RCTs indicated that in non-severe patients, CP has no benefit [58]; therefore, WHO recommended against CP utilizations in non-severe patients, but it can be used for critical patients within clinical trials [58].

Several Abs (e.g. B38, H4, CB6 and 4A8) have been isolated from convalescent COVID-19 individuals. The B38 and H4 Abs blocked RBD-ACE2 binding and decreased virus titers in infected lungs (*in vivo*) [59]. The CB6 Ab interferes with the virus-receptor interaction and neutralizes SARS-CoV-2 *in vitro* [60]. On the other hand, the 4A8 mAb does not block the S–ACE2 interaction, but showed high neutralization potency against the authentic and pseudotyped virus *in vitro* [61].

Memory B-cells specific for SARS-CoV-2 can be isolated from convalescent COVID-19 individuals and used to identify/clone mAbs [62]. Cloned mAbs bind specifically to RBD, block the RBD–ACE2 interaction, and neutralize pseudotyped virus infection [62]. Three RBD-specific mAbs (P2C-1F11, P2B-2F6 and P2C-1A3) demonstrated potent neutralization of live virus [63]. Pinto et al. described mAbs, such as S309, that target SARS-CoV-2 S glycoprotein [64]. The S309 mAb demonstrated potent authentic and pseudovirus neutralization [64]. Notably, the neutralization was enhanced by Ab cocktails that contain S309 [64].

In comparison with the original strain, the neutralization potency of CP against variants is significantly decreased [45].

The Omicron variant successfully escapes Abs that were induced by infection with previous variants, which indicates that CP may not be effective [26]. Ma et al. revealed that in comparison with the wild-type strain with D614G mutation, the 1-year post-infection CP demonstrated a reduction in neutralization activity against the Omicron (10.15-fold) and Delta (1.79-fold) variants [65]. Notably, there was a much greater decrease in neutralization activity against the Omicron variant [65] .

Previously, Ab phage-display libraries from recovered COVID-19 patients were used to isolate Abs that have shown potent neutralization of certain variants (picomolar doses) [66]. The NE12 Ab neutralizes the Alpha and Delta variants, while the NA8 Ab neutralizes the Beta and Omicron variants [66]. Additionally, in a golden Syrian hamster model, the NE12 and NA8 Abs demonstrated preventative and therapeutic efficacy [66].

However, there are many challenges with the use of CP treatment that require further evaluation [35]. Challenges include insufficient donor availability, health condition of donors, viral kinetics, variability between different batches of plasma, and host interactions of SARS-CoV-2 [35]. Notably, the variability between one batch of CP and another batch leads to several levels of success (low–high), which limits treatment reliability [9].

Antibodies such as mAbs, functional antigen-binding fragment (Fab), and single-chain variable region fragment (scFv) can be used to prevent and treat infections [67]. These scientifically generated Abs can be developed to target S1-RBD, S1 N-terminal domain (NTD), and the S2 region [67]. Therefore, viral infection can be inhibited by Abs blocking RBD-receptor binding as well as impeding S2-mediated membrane fusion and viral entry [67].

Previously, Abs have been developed against SARS-CoV-1 and MERS-CoV [67]. *In vitro* and *in vivo*, SARS-CoV-1 Abs demonstrated strong neutralizing activity, but these Abs have not been evaluated in clinical studies [67]. Similarly, the majority of the MERS-CoV Abs still need to be evaluated in clinical studies [67].

Notably, SARS-CoV-2 and SARS-CoV-1 have a ± 79% similarity and a high S protein sequence identity [2, 67]. Therefore, scientists have investigated the potential cross-reactivity and cross-neutralizing activity of SARS-CoV-1 Abs against SARS-CoV-2 infection [35, 67]. Both m396 and CR3014 are potent SARS-CoV-1-specific Abs that target the ACE2 binding site [68], but these Abs do not bind to the SARS-CoV-2 S protein [68]. On the other hand, the SARS-CoV-1 Ab CR3022 does bind to the SARS-CoV-2 S protein with high affinity [68].

Wang et al. produced a human 47D11 mAb and showed that it strongly inhibits SARS-CoV-2 S pseudotyped vesicular stomatitis virus (VSV) infection and neutralizes authentic infection *in vitro* [69]. Thereafter, a clinical trial demonstrated that an mAb cocktail significantly decreased hospitalization and deaths associated with COVID-19 [9]. Subsequently, the FDA authorized three mAb cocktails for emergency use in individuals infected with SARS-CoV-2 and at high risk for developing detrimental COVID-19 [9].

Several mAbs have shown to be effective in the treatment of SARS-CoV-2 infection, including bamlanivimab, regdanvimab, etesevimab, cilgavimab, tixagevimab, casirivimab, and imdevimab [26]. Most mAbs target/inhibit the S protein RBD [6], and variants, especially the Omicron variant, [18] have several S protein mutations [26]. These alterations change the binding of Abs to variants, which may affect their neutralization capabilities and allow variants to resist mAb neutralization [26].

The FDA has approved certain mAbs for emergency utilization to treat COVID-19 patients who may progress to severe disease [6]. These mAbs include bamlanivimab plus etesevimab, casirivimab plus imdevimab (REGEN-COV$_{TM}$), sotrovimab, and tixagevimab plus cilgavimab (Evusheld) [6].

REGEN-COV™ is beneficial for targeting variants and decreasing immune escape [20]. In a phase III trial, REGEN-COV™ treatment led to a 70% decrease in hospitalization/death of COVID-19 patients [20]. In adults and pediatric COVID-19 patients, REGEN-COV™ is FDA approved for the treatment of mild to moderate disease that has a high risk of developing into severe disease [20]. REGEN-COV™, and bamlanivimab + etesevimab treatments demonstrated efficacy against previous variants of concern, but decreased or no neutralization activity against the Omicron variant [45].

Previously, the bamlanivimab (LY-CoV555) and etesevimab (LY-CoV016) Ab cocktail was approved for emergency use [15]. Mutations at the S protein positions 484 and 417 have been related to immune evasion [15]. The Beta and Gamma variants were shown to escape neutralization by bamlanivimab due to the E484K mutation and etesevimab due to the K417N/T [70] mutation. The E484A and K417N mutations are also present in the Omicron variant, thus it may also be resistant to these Abs [15].

High-potency medications are required that target several SARS-CoV-2 variants [26]. Previously, mAb neutralization activity against variants was assessed by a live-virus focus reduction neutralization assay (FRNT) [71]. The Omicron variant was not neutralized by etesevimab, bamlanivimab and imdevimab [71], while casirivimab demonstrated a much lower level of Omicron variant neutralization compared with other variants [71]. The tixagevimab (COV2-2196), cilgavimab (COV2-2130), and sotrovimab (S309) Abs showed neutralization activity against the Beta, Gamma and Omicron variant [71]; however, activity against the Omicron variant was at a much higher concentration [71]. Cilgavimab and tixagevimab showed a 43-fold decrease in neutralizing potency against the Omicron variant [45].

The binding of sotrovimab (S309) or Evusheld were not influenced by the Omicron variant mutations [26]. Furthermore, sotrovimab has demonstrated effectiveness against the Omicron variant (*in vitro*) [26]. The neutralization activity of certain mAbs is based on targeting regions outside of the RBD or conserved epitopes, which allows the maintenance of effectiveness against several variants [26], e.g. sotrovimab, S2X259, and S2H97 targeting conserved epitopes and neutralizing the Omicron variant [26]. Notably, the authorized mAb treatments for Omicron are sotrovimab and Evusheld [6].

Most mAbs target the RBD, which can have various mutations depending on the SARS-CoV-2 variant [25]. The Omicron variant has several S RBD mutations, which indicates its potential to escape mAb neutralization [15]. Mutations allow the variants, especially Omicron, to resist mAb neutralization, thus decreasing mAb efficacy [25]. Notably, utilizing mAbs overcomes the challenges with serum therapy due to mAb specificity, purity, and safety [35].

Although Abs may be beneficial, some limitations and challenges are experienced with the use of Abs (large size, fragile, elevated immunogenicity) (Fig. 2) [72].

mAb treatments can be useful for patients experiencing mild COVID-19 symptoms [16]. However, due to the small amount of Ab reaching the target area, large repetitive Ab doses and intravenous administration by healthcare professionals are needed for effective [5] preventative/therapeutic effects [16]. This may indicate the low efficiency of intravenous Ab delivery because these large Abs will need to move through the plasma–lung barrier in order to treat lung infections [5]. Additionally, Abs usually only target one epitope at a time [16]. The modification and production of an Ab to contain various specificities is a slow and strenuous process that affects yield and quality [12]. Somatic mutations and Ab-dependent enhancement (ADE) are also challenges that may decrease Ab efficacy [7]. The emergence of numerous SARS-CoV-2 mutations is a big challenge for developing therapeutics [4]. Escape mutants can evade Ab

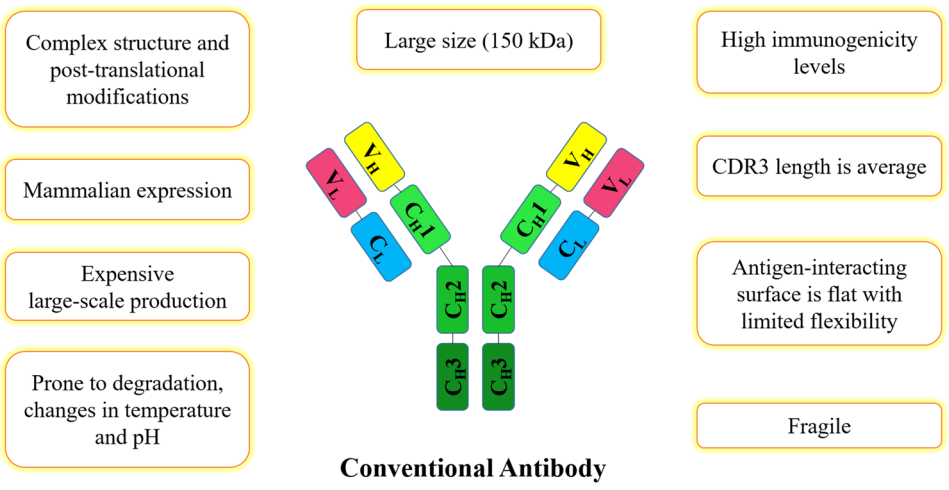

Fig. 2 Limitations and challenges with the utilization of conventional antibodies

neutralization and host protective immunity [4]. Notably, numerous anti-SARS-CoV-2 mAbs are ineffective against the Beta and Gamma variants [4].

Researchers are actively developing specific preventive and therapeutic strategies (vaccines, mAbs, IFN therapies) for COVID-19 [35]. Currently, some SARS-CoV-2-specific Abs are still under development [67]. Unfortunately, the development, evaluation (*in vitro* testing [neutralizing activity], *in vivo* testing [protective effectiveness], preclinical studies and clinical trials [safety and efficacy]) and approval of Abs for clinical application is a lengthy process (months or years) [35, 67]. Moreover, in previous animal models, clinical mAbs have been shown to be less efficient as a treatment than a prevention for COVID-19 [5].

Although mAbs can be beneficial, the various challenges, especially their large-scale, labor-intensive, lengthy and expensive production, overshadows their potential clinical application and limits global accessibility [5, 35]. Therefore novel therapies are required for diseases such as COVID-19 to decrease virus replication, virus spread, disease severity and fatality rates [35].

5 Nanobodies

Nanobodies (VHH or Nbs) are small monomeric antigen-binding fragments generated from heavy chain-only Abs that are present in camelids [72]. There are several advantages of Nbs, for example low toxicity, high affinity, sensitivity, water solubility, effortless production, prolonged shelf life, and many more (Fig. 3) [72].

Nbs can be successfully selected from different types of libraries (immune, naïve and synthetic) through several types of display technologies (phage, ribosome and yeast surface), and expressed in various expression systems (prokaryotic, eukaryotic and plants) [7]. Engineering multivalent, biparatopic and bispecific Nbs with greater efficiency is straightforward [12, 72]. Mature Nbs and multivalent Nbs can achieve substantial neutralization potency that is equivalent to, or greater than (per mass), certain effective SARS-CoV-2 mAbs [5]. Notably, the selection and large-scale production of specific Nbs can be achieved rapidly and inexpensively, which allows for high availability [72].

Nbs can be administered intravenously, intramuscularly, or subcutaneously, but inhalation delivery of Nb therapeutics is the most attractive option for COVID-19 [16]. In clinical specimens, SARS-CoV-2 viral copies was highest in the respiratory system, whereas levels in blood were low [73]. Moreover, systemic administration of mAbs results in low levels (0.2%) of the mAb dose reaching the lung [74]. This indicates that therapeutic agents delivered though inhalation would be more favorable than systemic administration [74]. In order for a treatment to be administered through pulmonary delivery, the treatment (e.g. Abs or Nbs) needs to be stable and to maintain structural integrity and bioactivity [74]. Notably, the various advantageous properties of Nbs (Fig. 3) can allow for successful Nb aerosolization [72] and Nbs may be formulated (nebulized spray) to be administered through inhalation for pulmonary delivery [7, 75]. This can be very beneficial regarding respiratory viruses because the treatment can be inhaled directly into lungs, allowing for greater treatment efficacy [75]. In addition, stable Nbs can

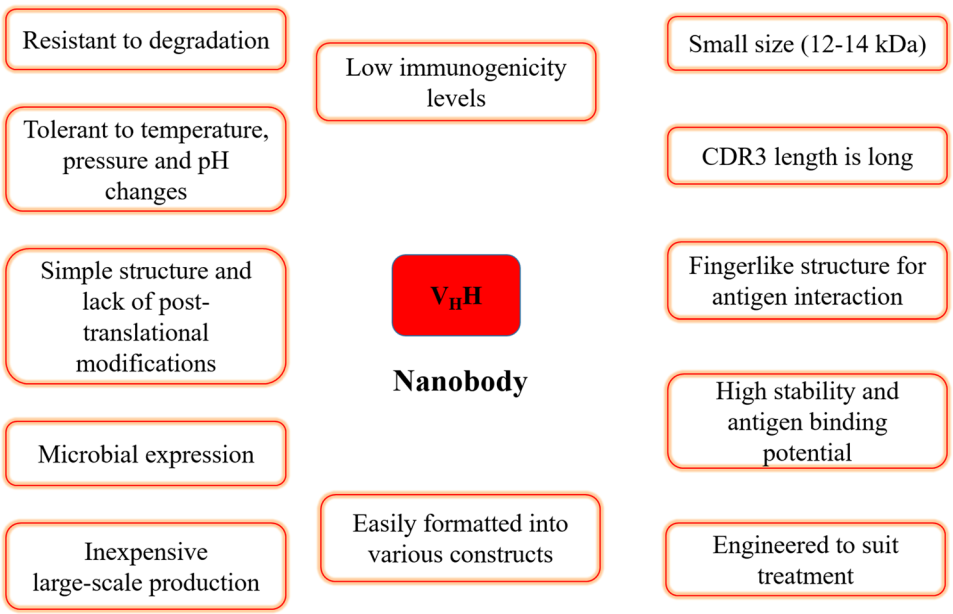

Fig. 3 Advantages of nanobodies

be engineered into disinfection products for COVID-19 prevention [76].

The various Nb properties indicate enhanced Nb capabilities [7] that can overcome many challenges experienced with Ab utilization. Thus, Nb development against SARS-CoV-2 can be very valuable [7] as the utilization of Nbs may lead to efficient targeted treatment delivery (aerosolization), which allows for high drug bioavailability, rapid onset of treatment, improved patient compliance and [5] self-administration.

Taken together, Nbs possess multiple favorable properties that translate into advantages in Nb drug development for COVID-19 prophylaxis, diagnostic and therapeutic purposes.

6 Nanobodies for the Diagnosis, Prevention and Treatment of COVID-19

The various Nb attributes offer a great opportunity for developing novel diagnosis and treatment interventions for COVID-19. Notably, over the past 3 years there has been a drastic increase in the generation and evaluation of Nbs targeting SARS-CoV-2 (Fig. 4). The literature was reviewed and the potential of several Nbs was noted, resulting in a comprehensive list of various Nbs as well as their diagnostic and therapeutic potential (see Table 3).

6.1 Nanobodies Against SARS-CoV-2 as a Diagnostic Option for COVID-19

Wagner et al. generated unique Nbs (NM1228, NM1226 and NM1230) that have a high RBD affinity (equilibrium dissociation constant [K_D] = 1.4–53 nM), potently block ACE2 binding to SARS-CoV-2 antigens (RBD, S1, and homotrimeric S protein) [NM1228 50% inhibitory concentration (IC_{50}) = 0.5 nM; NM1226 IC_{50} = 0.82 nM, and NM1230 IC_{50} = 2.12 nM] and neutralize infection *in vitro* (NM1226 IC_{50} ~ 15 nM, NM1228 IC_{50} ~ 7 nM, NM1230 IC_{50} ~ 37 nM and NM1224 IC_{50} ~ 256 nM)) [77]. A biparatopic Nb (NM1267) was generated by the fusion of two Nbs (NM1226 and NM1230) that simultaneously target two different RBD epitopes [77, 78]. The NM1267 demonstrated great improvements in RBD (wild-type and mutants) affinity (RBD wild-type (K_D ~ 0.5 nM) and RBD mutants (K_D ~ 0.6 nM for $RBD_{B.1.1.7}$; K_D ~ 1.15 nM for $RBD_{B.1.351}$), inhibition of ACE2 binding to antigens, and effective viral neutralization (IC_{50} ~ 0.9 nM) [77]. Most serological assays are unable to distinguish between total binding Abs and neutralizing Abs [77]. Currently, conventional virus neutralization tests (VNTs) are used to detect neutralizing Abs that need a biosafety level 3 (BSL3) laboratory, handling of infectious SARS-CoV-2 virions and excessive amounts of time (2–4 days) [77]. Wagner et al. used NM1267 to develop the NeutrobodyPlex, a competitive multiplex binding assay that detects neutralizing Abs and qualitatively and quantitatively evaluates the immune response in infected and vaccinated patients [77].

Various combinations of biotinylated Nbs (C5, F2, C1, H4) were evaluated as capture agents and probe agents in order to develop a sandwich ELISA for SARS-CoV-2 [22]. In the ELISA, the biotinx-C5-Fc (capture) and F2-Fc-HRP (probe) were shown to be an optimal combination with high specificity for S protein detection, which led to a limit of detection (LOD) of 514 pg mL^{-1} [22]. The use of site-selective biotinylation improved the ELISA sensitivity [22]. Using C5-Fc-SS-biotin as the capture showed increased sensitivity to the S protein (147–514 pg mL^{-1}) and RBD (33–85 pg mL^{-1}). Thus, a sensitive ELISA for SARS-CoV-2

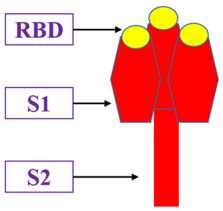

NANOBODIES FOR DIAGNOSIS

NM1267, C5, F2, VHH-72-13-C

NANOBODIES FOR PREVENTION

Nb_{15}-Fc, Nb_{22}-Fc, Nb_{31}-Fc

NANOBODIES FOR THERAPUTICS

VHH-72, H11-D4, H11-H4, Ty1, 1E2, 2F2, 3F11, 4D8, 5F8, 3F, 1B, 2A, Sb23, Nb3, Nb6, Nb11, Nb21, Nb20, Nb91, E, V, W25, MR3, MR17, HuNb11-59, PiN-21, WNb2, WNb7, WNb15, WNb36, aRBD-2-7, aRBD-2-5, Nb15, Nb19, Nb56, SP1D9, SP3H4, *Nanosota-1C*, SR6v15, C5, F2, Nb_{15}, Nb_{22}, and Nb_{31}, K-874A, NIH-CoVnb-112, Fu2, Nb1, Nb2, NM1267, NM1268, P2C5, P2G1, P5F8, saRBD-1, Sb#15, Sb#68, 7A3, 8A2, Nb-007, DL4, DL28, RBD-1-2G

Fig. 4 Nanobodies targeting the S protein (RBD, S1 and S2) for COVID-19 diagnosis, prevention and therapeutics. *RBD* receptor binding domain, *COVID-19* coronavirus disease 2019

detection was developed using Nbs, indicating the potential of Nbs in diagnostics [22].

The process of virus replication is facilitated by the replication transcription complex (RTC), which is assembled through various NSPs [79]. Notably, Nsp9 is essential for RTC assembly and function [79]. Esposito et al. identified 136 Nbs against Nsp9, and eight Nbs were selected for expression and purification [79]. The 2NSP23 and 2NSP90 Nbs were shown to bind and specifically recognize wild-type Nsp9 at low antigen concentrations (1.25 ng μL^{-1}) [79]. Moreover, both 2NSP23 and 2NSP90 Nbs were shown to specifically bind and detect Nsp9 in saliva from COVID-19 patients at low concentrations (about 10 ng) [79]. Therefore, the 2NSP23 and 2NSP90 Nbs may be useful to rapidly identify SARS-CoV-2-infected individuals indicating its diagnostic potential [79].

Gransagne et al. generated Nbs that target, specifically recognize and bind with high affinity (K_D = 0.206–46.5 nM) to the N protein [80]. The Nbs D12-3, E7-2, E10-3, G9-1 and H3-3 recognize the C-terminal domain (CTD), while NTD E4-3 and NTD B6-1 recognize the NTD [80]. Affinity binding was highest for E7-2 (K_D = 0.206 nM) and lowest for NTD B6-1 (K_D = 46.5 nM). In infected cell extracts, Nbs recognized the N protein, with signals ranging from 4 ng/mL (E7-2) to 4 µg/mL (NTD-B6-1). For N detection, Nbs against CTD were used in combination with anti-NTD Nbs to determine the optimal pairing. The Nb pairing of G9-1 and NTD-E4-3 produced the best signals (4 ng/mL), while the NTD E4-3 and G9-1 Nbs detected the N protein in B.1.351- and P1-infected mice. In infected cell extracts (Wuhan, B.1.1.7 and B.1.351 variants), the NTD E4-3 and G9-1 Nbs recognized the N protein. In infected FRhK4 cells and Syrian hamsters lung tissue, these Nbs were shown to identify the virus [80]. A specific and sensitive sandwich ELISA was developed using the NTD E4-3 and G9-1 Nbs [80]. Notably, the ELISA was shown to detect N protein in human nasopharyngeal swab samples [80]. In addition, NTD E4-3 and G9-1 were shown to detect SARS-CoV-2 variants [80].

6.2 Nanobodies Against SARS-CoV-2 as a Prevention Option for COVID-19

Previously, Nbs were produced against the major histocompatibility class (MHC) II complex antigens (VHH_{MHCII}) [81]. Thereafter, Pishesha et al. combined VHH_{MHCII} with SARS-CoV-2 S RBD ($Spike_{RBD}$) to develop a recombinant protein vaccine (VHH_{MHCII}-$Spike_{RBD}$) [82]. Mice immunized with VHH_{MHCII}-$Spike_{RBD}$ (two doses, 20 µg) elicited strong binding and neutralizing Abs against SARS-CoV-2 as well as variants (Wuhan Hu-1+D614G) [82]. Additionally, prominent CD8 T-cell responses were prompted by immunization [82]. Notably, the VHH_{MHCII}-$Spike_{RBD}$ vaccine showed stability at room temperature, retained efficacy after lyophilization, and was produced in high yields [82]. Hence, Nbs are a promising option for vaccine development.

Worldwide, approximately 51% of the population are not completely vaccinated [83]. About 1 month is required post-vaccination for complete inoculation and effective protection [83]. Thus, short-term instantaneous prophylaxis (STIP) is needed and can be beneficial for unvaccinated individuals [83]. The previously isolated Nb22 Nb showed ultra-potent neutralization of the Delta variant, bound to RBDs (original strain and Delta) and effectively blocked RBD-hACE2 binding [83]. Nb22-Fc interacted with the S protein of the WH01, D614G, Alpha, and Delta variants. The Nb22-Fc showed a higher neutralizing potency against the Delta variant (IC_{50} = 5.13 pM) compared with the WH01 (IC_{50} = 12.63 pM) and Alpha variants (IC_{50} = 43.13 pM). In post- and pre-exposure prophylaxis, intranasal Nb22 (average of 10 mg/kg) demonstrated protection against the Delta variant [83]. Notably in mice, intranasal Nb22 administration showed high efficacy against the Delta variant in STIP (7 days, single dose) and lengthy respiratory system retention (1 month, four doses) [83]. Additionally, Nb22 demonstrated *in vitro* room temperature stability (70–80°C, 1 h) and *in vivo* long-lasting retention.

6.3 Nanobodies Against SARS-CoV-2 as a Therapeutic Option for COVID-19

Huo et al. identified the H11 Nb and two affinity matured mutants of H11 (H11-D4 and H11-H4) [84]. The epitope targeted by H11-D4 and H11-H4 is directly next to and slightly overlaps the binding region of ACE2 [84]. Both H11-D4 and H11-H4 were shown to inhibit RBD and S from binding to ACE2 *in vitro* [84]. By surface plasmon resonance (SPR), RBD binding of H11-H4 had a K_D of 5 nM and H11-D4 had a K_D of 10 nM, whereas by isothermal titration calorimetry (ITC), RBD binding of H11-H4 had a K_D of 12 nM and H11-D4 had a K_D of 39 nM. Furthermore, Nbs can be fused to human IgG Fc domains [85]. The RBD binding was blocked by H11-H4-Fc (IC_{50} = 61 nM), H11-D4-Fc (IC_{50} = 161 nM) and VHH72-Fc (IC_{50} = 262 nM) *in vitro*. In addition, ACE2 binding was blocked by H11-H4-Fc (IC_{50} = 34 nM), H11-D4-Fc (IC_{50} = 28 nM) and VHH72-Fc (IC_{50} = 33 nM) *in vitro*. They were also shown to neutralize live virus, but H11-H4-Fc potency was greater [84]. The 50% neutralizing dose (ND_{50}) of the virus was 6 nM for H11-H4-Fc and 18 nM for H11-D4-Fc. CR3022 Ab and H11-H4 Nb recognize different epitopes on the RBD, and a combination of these two agents have shown additive virus neutralization [84].

The Ty1 Nb demonstrated specific and high-affinity RBD binding (K_D 5–10 nM), neutralization of pseudotyped viruses (Ty1: IC_{50} = 0.77 µg/mL; Ty1-Fc: IC_{50} of ~ 12 ng/mL), binding to RBD in the 'active' and 'inactive' states as well as

direct prevention of RBD–ACE2 binding [86]. For detection and diagnostic purposes, Ty1 can be utilized in flow cytometry and immunofluorescence [86]. For therapeutic purposes, large quantities of Ty1 can be produced fast and at a low cost [86].

Dong et al. produced multiple Nbs (e.g. 3F, 1B, 2A) that block the SARS-CoV-2–ACE2 interaction, and a combination of two Nbs showed synergistic blockage [85]. In order to improve S protein binding affinity, avidity, and blockage of the interaction, multiple different high-affinity Nbs that target different but adjacent RBD epitopes can be fused into a multispecific Nb [85]. Notably, at therapeutically relevant concentrations, S protein binding and blockade of the S–ACE2 interaction was significantly enhanced by the bi-specific Nb-fc (K_D = 0.25 nM, IC_{100} ~36.7 nM, IC_{95} ~12.2 nM, IC_{50} ~1 nM) compared with the monoclonal Nb-Fc [85]. The bi-specific 1B-3F Nb-Fc demonstrated increased binding to S1 RBD and S–ACE2 blockade [87]. 3F-Fc and 2A-Fc likely bind to different S1 RBD epitopes, whereas 1B-Fc and 2A-Fc may bind to the same S1 RBD [87] epitope. 3F-Fc does not compete with 1B-Fc or 2A-Fc, and likely binds to a different epitope [87]. Thereafter, several tri-specific Nb-Fc were constructed that demonstrated a further enhancement in efficacy [87]. The tri-specific Nb-Fc, 3F-1B-2A, showed extremely strong binding of S1 RBD, blockage of the S–ACE2 interaction and inhibition of pseudovirus infection *in vitro* [87]. *In vitro*, tri-specific Nbs (3F-1B-2A [K_D ~0.047 nM] and 1B-3F-2A [K_D ~0.095 nM]) demonstrated higher binding affinities to S1 RBD than 1B-3F [87]. Additionally, tri-specific Nbs (3F-1B-2A [0.71 nM], 1B-3F-2A [0.74 nM], and full inhibition [10 nM]) blocked the S–ACE2 interaction to a greater extent than mono-specific Nb-Fcs in combination (IC_{50} = 2.21 nM, and full inhibition around 100 nM) [87]. Similarly, the tri-specific Nb-Fcs (3F-1B-2A, IC_{50} = 3.00 nM; and 1B-3F-2A, IC_{50} = 6.44 nM) neutralized pseudovirus infection more effectively than the combination of VHH-Fcs (1B, 3F and 2A, IC_{50} = 29.19 nM) [87].

Three sybody (Sb) libraries (concave, loop and convex) were used to rapidly select various Sbs against SARS-CoV-2 RBD [88]. The potent Sb23 showed high RBD binding affinity (K_D = 10 nM) and effectively neutralized pseudovirus (IC_{50} = 0.6 µg/mL) [88]. Notably, the RBD affinity (K_D = 225 pM) and neutralization efficiency (~ 100-fold, IC_{50} = 0.007 µg/mL) was drastically enhanced by the bivalent Sb23-Fc construct [88]. Sb23 showed higher RBD affinity than ACE2, competes with ACE2 for RBD binding sites, and binds to RBD in the 'up' and 'down' conformation, therefore effectively blocking the SARS-CoV-2–ACE2 interaction [88]. Additionally, Sb23 could be combined with other Sbs (Sb12, 76, and 100) that simultaneously bind RBD and decrease ACE2 binding affinity [88].

Previously, synthetic Nbs that effectively disrupt the S–ACE2 interaction and inhibit pseudovirus infection were produced [11]. Nb6 and Nb11 targeted the RBD and impeded ACE2 binding, while Nb3 targeted different epitopes and reduced the S–ACE2 interaction. Nb6 binds to $Spike^{S2P}$ (K_D = 210nM) and to RBD alone (K_D = 41 nM), whereas Nb3 binds to $Spike^{S2P}$ (K_D = 61 nM), but there was no indication of binding to the RBD alone [11]. Nb6 and Nb11 were shown to be the most potent clones, with IC_{50} values of 370 and 540 nM, respectively. They recognize RBD epitopes overlapping the binding site of ACE2 [11] and bind to open and closed $Spike^{S2P}$ conformations. Pseudovirus infection was inhibited by Nb6 (IC_{50} = 2.0 µM), Nb11 (IC_{50} = 2.4 µM) and Nb3 (IC_{50} = 3.9 µM). Nb6 dimerization and trimerization lead to increases in K_D of 750-fold and K_D of > 200,000-fold, respectively. A trivalent Nb6 (Nb6-tri) Nb was generated to improve the affinity and inhibitory effects. The Nb6-tri was extremely potent and neutralized live SARS-CoV-2. Inhibition of pseudovirus infection was enhanced to a greater extent by Nb6-tri (2000-fold, IC_{50} = 1.2 nM) than Nb11-tri (40-fold, IC_{50} = 51 nM) and Nb3-tri (10-fold, IC_{50} = 400 nM). In the neutralization of live virus infection, Nb6-tri (IC_{50} = 160 pM) demonstrated greater potency than Nb3-tri (IC_{50} = 140 nM). Thereafter, potency was optimized by the selection of high-affinity mutations, which led to the production of a mature Nb6 (mNb6). The mNb6 showed enhanced binding affinity (500-fold affinity to $Spike^{S2P}$), inhibition of pseudovirus, and live virus infection (~ 200-fold). The inhibitory effects were further enhanced by the trivalent mNb6 (mNb6-tri), and the neutralization of SARS-CoV-2 is due to mNb6-tri locking S into an inactive format [11]. The mNb6-tri further enhances the inhibition of pseudovirus (IC_{50} = 120 pM or 5.0 ng/mL) and live infection (IC_{50} = 54 pM or 2.3 ng/mL). Interestingly, mNb6-tri was shown to remain stable and functional after heat treatment, lyophilization, and aerosolization. This indicates the potential of mNb6-tri to be aerosolically delivered directly into the lungs, which may allow for patient-friendly administration of a preventative/therapeutic drug against COVID-19 [11].

Three high-quality potent Nbs (Nb21, Nb20 and Nb89) demonstrated high affinities, pseudovirus neutralization, and thermostability (Nb89 = 65.9°, Nb20 = 71.8°, and Nb21 = 72.8°C) [89]. Interestingly, three copies of Nb20 or Nb21 showed simultaneous binding of all three RBDs in the inactive 'down' conformation [89]. The SPR showed the binding affinities of Nb89 (108 pM) and Nb20 (10.4 pM). Pseudovirus was neutralized by Nb89 (0.133 nM), Nb20 (0.102 nM), and Nb21 (0.045 nM). Moreover, live virus was neutralized by Nb89 (0.154 nM), Nb20 (0.048 nM), and Nb21 (0.022 nM). The Nb21 on-shelf stability after purification was ~ 6 weeks at room temperature. In comparison with the monomeric Nbs, the homotrimeric Nbs ($Nb21_3$ and $Nb20_3$) demonstrated an enhanced (~ 30-fold) inhibition of pseudovirus

($Nb21_3$, IC_{50} = 1.3 pM; and $Nb20_3$, IC_{50} = 4.1 pM) [89]. Notably, the multivalent constructs showed good physicochemical properties (solubility and thermostability) and high pseudovirus neutralization capabilities even after lyophilization and aerosolization, indicating the potential for aerosol-mediated administration [89]. Combining various multivalent constructs that are effective against SARS-CoV-2 could inhibit mutational escape [89].

Li et al. also produced several unique Sbs [90]. The potent MR3 binds the RBD (K_D = 1.0 nM), neutralizes the pseudovirus (IC_{50} = 0.40 μg mL^{-1}) and competes with ACE2 for RBD binding [90]. On the other hand, SR31 demonstrated high RBD binding (K_D = 5.6 nM) but no neutralizing activities [90, 91]. Yao et al. then revealed the potential of SR31 as a fusion partner for enhancing Nb potency [91]. Two modestly neutralizing Sbs (MR17 and MR6) were fused to SR31 [91]. In comparison with MR6 (K_D = 23.2 nM and IC_{50} = 77.5 nM) and MR17 (K_D = 83.7 nM and IC_{50}= 747 nM), the MR6-SR31 and MR17-SR31 conjugates were shown to substantially enhance RBD affinity (MR17-SR31: K_D = 0.3 nM; and MR6-SR31: K_D = 0.5 nM) and pseudovirus neutralization (MR17-SR31: IC_{50} = 52.8 nM and MR6-SR31: IC_{50} = 2.7 nM) [91].

Four Nbs (VHH E [K_D = 2 nM], VHH U [K_D = 21 nM], VHH V [K_D = 9 nM], and VHH W [K_D = 22 nM]) were shown to target the RBD and potently neutralized infection [12]. These Nbs showed good live virus neutralizing activity (IC_{50} = 48–185 nM). VHH E, which binds RBD in the 'up' conformation, was the most potent, and results suggest that VHH E induces the three 'up' conformations and causes the 'down' conformation to be inaccessible to the RBD [12]. Engineered multivalent Nbs (VHH EE and EEE) showed greater neutralizing activities (100 times) [12]. Both VHH EE and VHH EEE showed enhanced neutralization of the pseudotyped virus (EE IC_{50} = 930 pM; and EEE IC_{50} = 520 pM) and live wild-type virus (IC_{50} = 180–170 pM). Moreover, a mixture of two Nbs that bind to different epitopes demonstrated enhanced neutralization and prevention of replication [12]. Notably, biparatopic Nbs (VHH VE and EV) showed substantially higher (more than eight times) binding strength (VE [K_D = 84 pM] and EV [K_D = 200 pM]) and pseudotyped VSV neutralization (VE and EV, IC_{50} = 4.1–2.9 nM) than E alone [12]. Targeting two neutralizing epitopes simultaneously with biparatopic Nbs inhibits the emergence of escape mutants [12].

Gai et al. produced six Nbs that showed good binding capacity (K_D = 21.6–106 nM) to S RBD wild-type and eight mutants (Q321L, V341I, N354D, V367F, K378R, V483A, Y508H, and H519P), and also blocked the interaction between the eight mutants of RBD and ACE2 [92]. There were varying levels of RBD–ACE2 blocking activity for Nb8-87 (16.2%), Nb13-58 (50.4%), and Nb11-59 (98.9%). All Nbs had half maximal neutralization concentrations (EC_{50}) and IC_{50} values lower than 0.2 and 1 μg/mL, respectively. Notably, Nb16-68 (ND_{50} = 2.2 μg/mL) and Nb11-59 (ND_{50} = 0.55 μg/mL) demonstrated the most effective neutralizing activity against authentic virus [92]. The Nb11-59 was humanized (HuNb11-59) and expressed in *Pichia pastoris*, which produced extremely large amounts (20 g/L titer) of HuNb11-59 in minimal time (213 h) [92]. Thereafter, HuNb11-59 showed high purity (99.36%), great stability, and neutralization activity, indicating potential inhalation delivery and successful commercialization [92].

The Pittsburgh inhalable Nb 21 (PiN-21) is an extremely potent homotrimeric construct that demonstrated efficient prevention of SARS-CoV-2 infection *in vitro* [5]. In the respiratory tract of Syrian hamsters, intranasal PiN-21 (0.6 mg/kg) delivery substantially inhibited viral replication [5]. Therefore, the beneficial effects of PiN-21 *in vitro* was also seen *in vivo* [5]. Aerosol PiN-21 (~ 0.2 mg/kg) delivery extremely decreased viral load and prevented pneumonia and lung damage in Syrian hamsters [5]. Thus, human-to-human virus transmission may be restricted by aerosol-mediated Nb administration [5]. The administration of PiN-21 through inhalation at an early stage of disease was shown to effectively reduce virus entry and replication, indicating disease prevention [5]. Thus, PiN-21 showed great efficacy for the prevention and treatment of COVID-19 [5].

Pymm et al. identified several high affinity Nbs (WNb 2, WNb 7, WNb 15, and WNb 36 [K_D = 0.14–19.49 nM]) that disrupted the RBD–ACE2 interaction and neutralized the virus (3–36108 nM) [17]. The Nb-Fc fusions bind to distinct antigenic sites on RBD (nM), inhibit ACE2–RBD interaction, and bind to most RBD variants (EC_{50} 0.7–14 nM). Nb-Fc (WNb 2, 7, 15, and 36) binds to wild-type RBD (EC_{50} = 0.97–2.65 nM), but showed decreased binding to either E484K or N501Y variant RBDs. The Nb-Fc fusions bind to wild-type RBD and the N501Y variant at K_D < 0.55 nM. The Nb-Fc 2 inhibited wild-type (IC_{50} = 0.16–0.61 nM) and most RBD variants (IC_{50} = 0.04–1.8 nM) and RBD–ACE2 engagement. The potent Nb-Fcs were shown to impede the interaction between variants (N501Y, and to a greater extent, E484K [IC_{50} = 0.04–0.19 nM]) RBD and ACE2 and potently neutralize SARS-CoV-2 (wild-type [IC_{50} = 0.10–3.18 nM] and N501Y D614G [IC_{50} = 0.11–5.04 nM] variants) [17]. Additionally, in N501Y D614G variant-infected mice, prophylactic Nb-Fc (alone or in combination) administration decreased viral loads, indicating their potential for COVID-19 prevention [17].

VHH-72 Nb was generated against SARS-CoV-1 RBD, however VHH-72 was able to cross-react with the SARS-CoV-2 RBD [75]. VHH-72 binds to SARS-CoV-1 RBD with an affinity of 1.2 nM, whereas for SARS-CoV-2 RBD, the K_D was ~ 39 nM. The VHH-72 Nb was shown to competitively [14] bind RBD with high affinity, however its

neutralization of S pseudotypes was at a high IC_{50} [75]. Therefore, the bivalent VHH-72-Fc was constructed and showed enhanced RBD binding affinity as well as neutralization of SARS-CoV-2 pseudoviruses at a low IC_{50} of 0.2 µg/mL [75]. In comparison with CR3022, VHH-72 prevents ACE2–SARS-CoV-2 binding [75]. Thereafter, multivalent VHH-72 Nbs were engineered in order to enhance neutralization activities [14]. The VHH-72 demonstrated binding affinity (K_D = 29–60 nM) for wild-type and variants (UK and SA). The tetravalent and hexavalent VHH-72 demonstrated substantial synergistic increases in neutralization efficacy [14]. The neutralization potency of VHH-72 increased with the increase in valency, as seen with the bivalent VHH-72 (IC_{50} = ± 3.3 nM), the tetravalent (IC_{50} = ± 0.34 nM) and the hexavalent (IC_{50} = ± 0.035 nM) against the wild-type. Notably, the hexavalent VHH-72 demonstrated potent pseudovirus neutralization of the UK (IC_{50} = ± 0.31 nM) and SA (IC_{50} = ± 0.072 nM) variants as well as the wild-type [14]. Interestingly, the neutralizing potency of the multivalent VHH-72 could be greater than the S309 (IC_{50} = ± 1.9 nM) mAb [14]. In addition, the multivalent VHH-72 Nbs demonstrated advantageous biophysical properties (low off-target binding, high stability and solubility), indicating their potential as therapeutic agents [14].

The *Nanosota-1A* Nb showed excessive neutralization potency, and affinity maturation resulted in *Nanosota-1B* and then *Nanosota-1C* [48]. *Nanosota-1A*, *-1B*, *and -1C* bind RBD with increasing affinity (K_d = 228–14 nM) and effectively inhibit viral infection *in vitro*. Furthermore, *Nanosota-1* strongly neutralizes pseudoviruses bearing the D614G mutation [48]. *Nanosota-1C* was shown to access the S protein in the accessible and inaccessible states [48]. Both *Nanosota-1C* and *Nanosota-1C-Fc* compete with ACE2 to bind RBD [48]. In order to inhibit the virus–ACE2 binding, a Nb needs to bind to RBD more strongly than ACE2 [48]. In comparison with ACE2, *Nanosota-1C-Fc* did in fact bind more strongly. Notably, *Nanosota-1C-Fc* binds RBD with the highest affinity (K_d = 15.7 pM) and ~ 3000 times tighter than ACE2 [48]. Both *Nanosota-1C-Fc* and *Nanosota-1C* potently inhibited pseudovirus entry as well as live virus infection [48]. *Nanosota-1C-Fc* demonstrated potent pseudovirus neutralization (ND_{50} = 0.27 µg/mL and ND_{90} = 3.12 µg/mL), which was ~ 10 times greater than *Nanosota-1C* and ~ 160 times greater than ACE2. *Nanosota-1C-Fc* also potently neutralizes live virus infection (ND_{50} = 0.16 µg/mL), again to a greater extent than *Nanosota-1C* and ACE2. *In vivo*, in hamster and mouse models, *Nanosota-1C-Fc* (10–20 mg/kg) showed preventive as well as therapeutic effectiveness against SARS-CoV-2 live infection [48]. Additionally, *Nanosota-1C-Fc* demonstrated exceptional thermostability (−80°C, 4°C, 25°C, or 37°C for 1 week), *in vivo* stability (10 days) and tissue bioavailability (after 3 days) [48]. Therefore, *Nanosota-1C-Fc* may be an effective and inexpensive treatment against COVID-19 [48].

Huo et al. produced four Nbs (C5, H3, C1, F2) with high binding affinity (K_D = 20–615 pM) and demonstrated that ACE2 binding was blocked by C1, H3 and C5, whereas it was unaffected by F2 [93]. C1 and F2 were shown to bind to the Alpha, Beta and Victoria strains at similar affinities, whereas C5 and H3 were shown to bind to only the Alpha and Victoria strain, and not the Beta strain. [93]. The C5 binds to RBD (K_D = ± 210 pM) and S (K_D = ± 350 pM) with high affinity and neutralized the Victoria (IC_{50} = 18 pM) and Alpha (IC_{50} = 25 pM) strains. The C1 was active against the Beta strain. Trimeric (C5, C1 and H3) Nbs bind to RBD at an enhanced K_D (10- to 100-fold) and showed potent virus (Victoria, Alpha or Beta strains) neutralization [93]. The C5 trimer showed enhanced neutralization potency against the live Victoria strain (ND_{50} = 3 pM), and C5-Fc showed RBD binding affinity (K_D = 37 pM) and virus neutralization potency (ND_{50} = 2 pM) similar to the trivalent C5. Regarding RBD binding, C1 and F2 competed with CR3022, whereas C5 and H3 competed with H11-H4. In the Syrian hamster model, intraperitoneal (IP) administration of C5-Fc (4 mg/kg) showed therapeutic efficacy [93]. Additionally, in the hamster model, IP and intranasal administration of the trimeric C5 Nb showed therapeutic benefit [93].

Wu et al. isolated three Nbs (Nb_{15}-Fc, Nb_{22}-Fc, and Nb_{31}-Fc) that showed specific RBD binding (K_D = 1.13–1.76 nM) and potent neutralization of SARS-CoV-2 (live virus [IC_{50} = 41.3–75 pM and IC_{90} = 195–293.8 pM] and pseudovirus [IC_{50} = 10–28.8 pM]) [74]. The three Nb-Fcs did not inhibit MERS-CoV or SARS-CoV pseudovirus. Interestingly these Nb-Fcs inhibited 15 SARS-CoV-2 variants. All three Nb-Fcs inhibited the replication of SARS-CoV-2 variants with a D614G mutation. Notably, the bivalent Nb_{15} (IC_{50} = 11 pM), trivalent Nb_{15} (IC_{50} = 9.0 pM), and tetravalent Nb_{15} (IC_{50} = 4.3 pM) showed enhanced neutralization potency compared with monomeric Nb_{15} (IC_{50} = 2.3 nM). Thereafter, a heterotrimeric and bispecific Nb (Nb_{15}-Nb_H-Nb_{15}) was engineered in order to enhance efficacy [74]. This construct contained a Nb specific for human serum albumin (HSA) [Nb_H] and two Nb_{15} specific for RBD [74]. Nb_{15}-Nb_H-Nb_{15} showed substantially elevated neutralization efficacy (pM) against wild-type and 18 mutant variants (*in vitro*), as well as excellent thermal stability (70–80°C, 1 h) [74]. Nb_{15}-Nb_H-Nb_{15} demonstrated specific RBD (K_D = 0.54 nM) and HSA (K_D = 7.7 nM) binding. Moreover, it was potent against the pseudotyped variants with D614G and N501Y mutations (UK and SA). Nb_{15}-Nb_H-Nb_{15} showed neutralization against the pseudotyped variants wild-type (IC_{50} = 9.0 pM), Alpha (IC_{50} = 5.9 pM) and Delta (IC_{50} =116 pM), but failed to neutralize the Gamma and Beta variants. Among various administration routes (intranasal, intraperitoneal, intravenous),

the intranasal Nb_{15}-Nb_H-Nb_{15} administration was the most favorable route, resulting in high and sustained (7 days) levels of Nb_{15}-Nb_H-Nb_{15} in lungs (*in vivo*) [74]. Notably, in transgenic human ACE2 (hACE2) mice, intranasal Nb_{15}-Nb_H-Nb_{15} (average of 10 mg/kg) administration showed substantial prophylactic and therapeutic efficiency against viral infection [74].

Guttler et al. produced various Nbs (e.g. Re6B06, Re9F06, Re5D06) that completely prevent infection [4]. Several of these Nbs demonstrated neutralization, hyper-thermostability, binding of S protein in the active and inactive states, and tight RBD binding [4]. Additionally, Nb tandems were constructed and Nb monomers were identified that keenly binds RBD which possess a mixture of escape mutations (K417T, E484K, N501Y, L452R), indicating high mutational tolerance [4]. Re5D06 (K_D ~2 pM), Re9B09 ($K_D \leq 1$ pM), Re6H06 ($K_D \leq 1$ pM), Re5F10 (~30 pM), Re9H01 (~10 pM), and Re9H03 (~25 pM) showed tight RBD binding. Some Nbs neutralize in the low nM range, such as Re9F06 (17 nM), Re5F10 (5 nM), Re6B07 (5 nM), and Re6B06 (50 nM), whereas other Nbs neutralize in the pM range, i.e. Re9B09, Re9H01, Re9H03 (167 pM), Re5D06 and Re6H06 (50 pM) [4]. Re5D06, Re6H06 or Re9B09 block the ACE2–RBD interaction, while Re5F10, Re7E02 or Re9F06 also competed with ACE2. Re9B09 and Re5D06, Re9F06 and Re5F10 are hyperthermostable (90°C, 5 min) or can robustly refold after heat treatment. The trimerization of Nbs decreased the minimal neutralization concentration (Re9F06 =167 pM; Re6D06 = 17 pM) [4]. The Re5D06–RBD model can accommodate the N501Y exchange, and the combination of mutations Beta (K417N, E484K, N501Y) or Gamma (K417T, E484K, N501Y) decreased the Re5D06–RBD interaction (K_D = 0.1–0.5 nM).

Fusion of Re9F06 to R28 lead to a tandem that binds rapidly to the Beta and Gamma variants. A quadruple (K417T, L452R, E484K, N501Y) RBD mutant that contains several mutations was produced. The Re9F06-R28 tandem was shown to bind to the mutated variants. Re6H06 showed ≤ 10 pM binding to either the Beta or Gamma, and Re9H03 binds mostly irreversibly to Gamma, Beta variants, and the quadruple mutant. Lastly, there was potent B.1.351 neutralization by monomers (Re5F10 [1.7 nM], Re6H06 [170 pM], Re9B09 [1.7 nM], Re9H03 [50–170 pM]) and tandems (Re9F06-R28 [50 pM], Re9F06-Re9B09 [50 pM], and Re9F06-Re6H06 [17 pM] [4].

The K-874A Nb was generated and binds specifically to the S1 protein with high affinity (K_d = 1.4 nM) and neutralizes the B.1.1.7 variant (IC_{50} = ± 5.74 µg/mL), but not the other variants [94]. Interestingly, the K-874A Nb does not reduce/prevent viral attachment to the ACE2 [94]. Instead, K-874A blocks the fusion between the virus membrane and the host cell, which inhibits viral entry [94]. In infected Syrian hamsters, intranasal administration of K-874A (30 mg/kg) was shown to decrease viral RNA copies in the lungs and inhibit the increase of cytokine levels [94].

Another biparatopic Nb (NM1268) was produced (NM1228 and NM1226) that targets different epitopes inside the RBD–ACE2 interface [78]. Both NM1267 and NM1268 showed strong RBD binding affinity. NM1268 demonstrated picomolar affinities to $RBD_{B.1}$, blockage of the ACE2–antigen interaction at low picomolar range, high stability and production at a high purity and yield [78]. Both biparatopic Nbs efficiently bind with high affinity to several variants (Alpha, Beta, Gamma, Delta) and were shown to neutralize the Beta and Delta variants *in vitro* [78]. NM1267 neutralized B.1 (IC_{50} = 0.33nM), B.1.351 (IC_{50} = 0.78 nM) and B.1.617.2 (IC_{50} = 52.55 nM). NM1268 showed strong neutralization potency for B.1 (IC_{50} = 2.37 nM), B.1.351 (IC_{50} = 6.06 nM), and B.1.617.2 (IC_{50} = 0.67 nM). Additionally, in K18-hACE2 mice, the prophylactic intranasal NM1267 and NM1268 Nb (20 µg) treatment was shown to inhibit virus-induced (B.1, B.1.351 or B.1.617.2) infection, virus shedding, disease progression and mortality [78]. Prophylactic NM1267 treatment decreased lung tissue damage induced by virus and inflammation in B.1-infected mice.

The potent NIH-CoVnb-112 Nb demonstrated strong binding affinity (4.9 nM) to S RBD and effectively interferes with the S RBD–ACE2 interaction with a EC_{50} of 0.02 µg/mL [95]. Notably, the affinity of monomeric NIH-CoVnb-112 was substantially better than other monomeric Nbs (VHH72, Ty1, Sb#14, and Sb23) [95]. In comparison with the S RBD wild-type, many variants of S RBD (N354D D364Y, V367F, and W436R) have shown extremely higher affinity for ACE2 (100-fold) *in vitro* [95]. Remarkably, NIH-CoVnb-112 binding affinity to these variants, as well as its ability to block the interaction between the variants and ACE2, were similar to its effects with the wild-type S RBD [95]. *In vitro*, pseudotyped lentivirus infection was shown to be blocked by NIH-CoVnb-112 [95]. Interestingly, NIH-CoVnb-112 and VHH-72 bind to different epitopes and their combination led to additive effects [95]. Post-nebulization of NIHCoVnb-112 showed that a large percentage (> 90%) of total input protein was recovered, it maintains effectiveness and there was no sign of degradation/aggregation products following exposure to physiological temperature (37°C, 24 h). NIH-CoVnb-112 also showed variant neutralization of Alpha (EC_{50} = 9.4 nM), Beta (EC_{50} = 15.8 nM), Gamma (EC_{50} = 17.6 nM), and Delta (EC_{50} = 14.5 nM) *in vitro* [95].

Table 2 Summary of the binding affinity of nanobodies, *in vitro* and *in vivo* efficacy

Nbs and Nb constructs	Binding affinity	Pseudovirus neutralization	Live virus neutralization	Prevention/ treatment *in vivo*	References
PiN-21				Intranasal (0.6 mg/kg) Aerosol (~ 0.2 mg/kg)	[5]
WNbFc 2, WNbFc 7, WNbFc 15, WNbFc 36	WNbFc fusions (K_D < 0.55 nM)		WNbFc (IC_{50} = 0.11–5.04 nM)	Intraperitoneal injection (5 mg/kg)	[17]
MR3 MR17 MR3-MR3 MR3-MR3-ABD	MR3 (K_D = 1.0 nM) MR17 (K_D = 83.7 nM) Fc-MR3 (K_D = 0.22 nM) Fc-MR17 (K_D = < 1 pM)	MR3 (IC_{50} = 0.42 μg mL^{-1}) Fc-MR3 (IC_{50} = 42 ng mL^{-1}) Fc-MR17 (IC_{50} = 0.46 μg mL^{-1}) MR3-MR3 (IC_{50} = 10 ng mL^{-1})		Intraperitoneal (2.5 mg)	[98]
SP1D9 SP3H4	SP1D9 (K_D = 8.9–49.7 nM)	SP1D9 (EC_{50} = 0.45 nM) SP3H4 (EC_{50} = 0.14 nM)	SP1D9 (EC_{50} = 1.12 nM) SP3H4 (EC_{50} = 0.70 nM)	Intraperitoneal injection (10 mg/kg)	[9]
Nanosota-1A, Nanosota-1B, Nanosota-1C, Nanosota-1C-Fc	(K_d = 14–228 nM) *Nanosota-1C-Fc* (K_d = 15.7 pM)	*Nanosota-1C-Fc* (ND_{50} = 0.27 μg/mL and ND_{90} = 3.12 μg/mL)	*Nanosota-1C-Fc* (ND_{50} = 0.16 μg/mL)	Intraperitoneal (10–20 mg/kg)	[48]
C5 C5-Fc Trimeric C5	C5 (K_D = ± 210–350 pM) C5-Fc (K_D = 37 pM)	C5 (IC_{50} = 18–25 pM)	C5 trimer (ND_{50} = 3 pM) C5-Fc (ND_{50} = 2 pM)	Intraperitoneal C5-Fc Intraperitoneal and intranasal trimeric C5 (4 mg/kg)	[93]
Nb_{15}-Fc, Nb_{22}-Fc, Nb_{31}-Fc, Nb_{15}-Nb_H-Nb_{15}	Nb_{15}-Fc, Nb_{22}-Fc, and Nb_{31}-Fc (K_D = 1.13–1.76 nM) Nb_{15}-Nb_H-Nb_{15}: (K_D = 0.54 nM)	Nb_{15}-Fc, Nb_{22}-Fc, and Nb_{31}-Fc (IC_{50} = 10–28.8 pM) Nb_{15}-Nb_H-Nb_{15} (IC_{50} = 5.9–116 pM)	Nb_{15}-Fc, Nb_{22}-Fc, and Nb_{31}-Fc (IC_{50} = 41.3–75 pM and IC_{90} = 195–293.8 pM)	Intranasal Nb_{15}-Nb_H-Nb_{15} (average of 10 mg/kg)	[74]
K-874A	(K_D = 1.4 nM)		(IC_{50} = ± 5.74 μg/mL)	Intranasal (30 mg/kg)	[94]
NIH-CoVnb-112	(K_D = 1.59–4.28 nM)	(EC_{50} = 9.4–17.6 nM)		Nebulization (25 mg/mL)	[95, 96]
Fu2 Fu2-Fc Fu2-Ty1 Fu2-Alb1		Fu2 (IC_{50} = 7 nM) Fu2-Fc and Fu2 homodimer (IC_{50} = 0.75–0.8 nM) The Fu2-Ty1 (IC_{50} = 140 pM)	Fu2 (N_{50} = 6.1 μg/mL) Fu2-Fc (N_{50} = 570 ng/mL) Fu2 dimer (N_{50} = 57 ng/mL)	Intraperitoneal injection Fu2-Alb1 (600 μg per day, 1–6 days)	[99]
NM1267 NM1268	(K_D = ~ 0.5 nM)	NM1268: (IC_{50} = 2.37–6.06 nM) NM1267: (IC_{50} = 0.33–52.55 nM)		Intranasal (20 μg)	[77, 78]
ABS-VIR-001	(K_D = 2.49E10 M)			Intraperitoneal and intranasal (10–25 mg/kg)	[100]
7A3 8A2	7A3 (K_D = 0.96 nM) 8A2 (K_D = 0.8 nM)	8A2 (IC_{50} = 5 nM) 7A3 + 8A2 (IC_{50} = 1.6 nM)	7A3 + 8A2 (IC_{50} = 0.14–27 nM)	Intraperitoneal 7A3 V_HH-hFc or 7A3+8A2 (5 mg/kg)	[97]
aRBD-2-5-Fc aRBD-2-7-Fc	aRBD-2-5-Fc (K_D = 12.3 pM) aRBD-2-7-Fc (K_D = 0.22 nM)	aRBD-2-5-Fc (IC_{50} = 0.051–0.108 nM) aRBD-2-7-Fc (IC_{50} = 0.032–0.191 nM)	aRBD-2-5-Fc and aRBD-2-7-Fc (IC_{50} = 0.027–0.129 nM)	Intraperitoneal aRBD-2-5-Fc (10 mg/kg)	[101]

Nbs nanobodies, K_D dissociation constant, IC_{50} 50% inhibitory concentration, EC_{50} half maximal effective concentration, ND_{50} 50% neutralizing dose

Table 3 Nanobodies generated against SARS-CoV-2 and their potential in COVID-19 diagnosis as well as treatment

Nbs and Nb constructs	Source	SARS-CoV-2 target	Nbs for diagnostics	Date and reference
E2, B6, C2, E2−B6, E2−C2, Bt-C2−B6	llama immunization and phage display	N protein	*Inhibition route* Each Nb binds to a specific epitope on the N High-affinity binding (K_D = sub-nM) *Utilization for detection* E2 was the best capture, with B6 or C2 as tracers E2−B6 and E2−C2: improved capturing Sandwich assays for N detection: best results with E2−B6 and E2−C2 as captures and Bt-C2−B6 as tracers Low LOD (50 pg/mL)	May 2021 [102]
NM1228 NM1226 NM1230 Biparatopic Nbs NM1267 NM1268	Alpaca immunization	RBD	*Inhibition route* High RBD affinity (K_D = 1.4–53 nM) Effectively block SARS-CoV-2 antigens (RBD, S1, S) binding to ACE2 (NM1228 [IC_{50} = 0.5 nM], NM1226 [IC_{50} = 0.82 nM] and NM1230 [IC_{50} = 2.12 nM]) NM1228 and NM1226 were unable to bind simultaneously, suggesting that NM1228 and NM1226 recognize similar or overlapping epitopes *Inhibition of pseudovirus* Neutralization of infection (SARS-CoV-2-mNG infectious clone) *in vitro* (NM1226 [IC_{50} ~ 15 nM], NM1228 [IC_{50} ~ 7 nM], NM1230 [IC_{50} ~ 37 nM] and NM1224 [IC_{50} ~ 256 nM]) *Inhibition route* Biparatopic Nbs: enhanced affinities for RBD wild-type (K_D ~ 0.5 nM) and RBD mutants ($RBD_{B.1.1.7}$ K_D ~ 0.6 nM, $RBD_{B.1.351}$ K_D ~ 1.15 nM) Biparatopic Nbs: inhibition of ACE2 binding to RBD, S1, and S (IC_{50} = low pM) *Inhibition of pseudovirus* NM1267 (IC_{50} ~ 0.9 nM) showed increased viral neutralization NM1267: targets different RBD epitopes Enhanced RBD (wild-type and mutants, Alpha Beta, Gamma, Delta) affinity, inhibition of ACE2–antigen binding and effective neutralization NM1267: neutralization of B.1 (IC_{50} = 0.33nM), B.1.351 (IC_{50} = 0.78 nM) and B.1.617.2 (IC_{50} = 52.55 nM) *Utilization for detection* NeutrobodyPlex developed using NM1267. Allows for neutralizing Abs detection and immune response evaluation	May 2021 [77]
Biotinx-C5-Fc F2-Fc-HRP	–	–	*Utilization for detection* High specificity for S protein detection in an ELISA The optimal combination was $biotin_x$-C5-Fc (capture agent) and F2-Fc-HRP (probe agent) [LOD = 514 pg mL^{-1}] Site-selective biotinylation decreased LOD C5-Fc-SS-biotin (capture) had increased sensitivity to S protein (147–514 pg mL^{-1}) and RBD (33–85 pg mL^{-1})	September 2021 [22]
2NSP23, 2NSP90	llama immunization	Nsp9 protein	*Inhibition route and utilization for detection* Specific recognition and binding to wild-type Nsp9 at low antigen concentrations (1.25ng μL^{-1}) Specific binding and detection of Nsp9 in saliva at low concentrations (about 10 ng) Nbs stabilize a tetrameric Nsp9 form that is incompatible with an Nsp9 monomeric form within the RTC complex Inhibition of viral replication	December 2021 [79]
D12-3, E7-2, E10-3, G9-1, H3-3, NTD E4-3, NTD B6-1	Alpaca immunization and phage display	N protein	*Inhibition route* Specific recognition of N protein *in vitro* and *in vivo* Strong binding and high affinity (K_D = 0.206–46.5 nM) Affinity binding to N was highest for E7-2 (K_D = 0.206 nM) and lowest for NTD B6-1 (K_D = 46.5 nM) E7-2, G9-1, and H3-3 recognize overlapping epitopes NTD B6-1 and NTD E4-3 recognize different epitopes *Utilization for detection* In infected cell extracts, Nbs recognized the N protein, with signals ranging from 4 ng/mL (E7-2) to 4 µg/mL (NTD-B6-1) Developed an ELISA to recognize the N protein, which included NTD E4-3 and G9-1 (optimal pairing) and produced the best signals (4 ng/mL) ELISA detects the virus in human nasal swabs NTD E4-3 and G9-1 also detects variants (B.1.1.7/alpha, B.1.351/beta) The NTD E4-3 and G9-1 Nbs detect the N protein in B.1.351- and P1-infected mice In infected cell extracts (Wuhan, B.1.1.7, and B.1.351 variants), NTD E4-3 and G9-1 Nbs recognized the N protein	January 2022 [80]

Table 3 (Continued)

Nbs and Nb constructs	Source	SARS-CoV-2 target	Nbs for diagnostics	Date and reference
VHH-72-13C	–	–	*Inhibition route* High affinity for RBD (K_D = 12.1 nM) *Utilization for detection* Electrochemical COVID-19 detection device using an Nb Rapid detection of virus and variants (Alpha, Beta and Delta) in *in vitro* and clinical samples	May 2022 [103]
VHH_{MHCII}	Alpaca immunization	MHC II	Part of the VHH_{MHCII}-$Spike_{RBD}$ vaccine: VHH_{MHCII}-$Spike_{RBD}$ (20 μg) Vaccine elicits high titer anti-$Spike_{RBD}$ and neutralizing Abs in mice Vaccine (two doses) maintains high IgG titers against mutant $Spike_{RBD}$ (K417T, E484K, and N501Y) High binding Immunity against SARS-CoV-2 as well as variants (Wuhan Hu-1+D614G) Effective post lyophilization and manufactured in high yields	November 2021 [81, 82]

Nbs and Nb constructs	Source	SARS-CoV-2 target	Nbs for prevention and vaccines	Date and reference
			Strong humoral response regardless of administration route (intraperitoneal, intramuscular, and intranasal), storage temperature, and formulation In a mouse model, humanized VHH_{hMHCII}-$Spike_{RBD}$ elicits humoral and cellular immunity	
Nb_{15}-Fc Nb_{31}-Fc Nb_{22}-Fc	–	–	*Inhibition route* High affinity of Nb_{15}-Fc, Nb_{22}-Fc and Nb_{31}-Fc to the Delta variant RBD (0.31–1.86 nM) Nbs did not neutralize variants with the E484K/Q mutation Nb_{22}–RBD binding blocks hACE2–RBD binding during infection The binding site of Nb_{22} on RBD partially overlaps the hACE2 binding site *Inhibition of pseudovirus* Nb_{22}-Fc: Higher neutralizing potency against the Delta variant (IC_{50} = 5.13 pM) compared with the wild-type (IC_{50} = 12.63 pM) and Alpha variants (IC_{50} = 43.13 pM) Interacted with the S protein of wild-type, D614G, Alpha and Delta variants Nb_{22}-Fc had an increased (2.5- to 8.4-fold) neutralizing potency against the Delta variant (IC_{50} = 5.13 pM) compared with the WH01 (IC_{50} = 12.63 pM) and Alpha variants (IC_{50} = 43.13 pM) Effectively blocks RBD–hACE2 binding *Inhibition of in vivo infection* Intranasal administration (average of 10 mg/kg) showed high efficacy against the Delta variant in STIP *Properties* *In vitro* stability (70–80 °C, 1 h) and *in vivo* long-lasting retention	March 2022 [83]

Nbs and Nb constructs	Source	SARS-CoV-2 target	Nbs for neutralization and therapeutics	Date and reference
VHH-72 VHH-72-Fc	llama immunization	Prefusion stabilized SARS-CoV-1 and MERS-CoV S proteins	*Inhibition route* VHH-72 high RBD binding affinity to SARS-CoV-1 (1.2 nM) and SARS-CoV-2 (K_D ~ 39 nM). The binding angle of VHH-72 to RBD, the 'down' conformation, would clash with the S2 fusion subunit Once a VHH-72 binds, the bound protomer would be trapped in the 'up' conformation Trap RBDs in the 'up' conformation *Inhibition of pseudovirus* VHH-72-Fc elevated RBD binding affinity and SARS-CoV-2 pseudovirus neutralization (IC_{50} = 0.2 μg/mL)	May 2020 [75]
Single-domain Abs	Phage-displayed single-domain Ab library	Five epitopes on RBD	*Inhibition route* Specific high-affinity binding to RBD Binding to both S1 and RBD Effective pseudotyped and live virus neutralization	June 2020 [104]
H11 H11-D4 H11-H4 H11-H4-Fc, H11-D4-Fc	Naive llama Nb library and phage display	S RBD	*Inhibition route* Inhibit RBD-ACE2 and S-ACE2 binding *in vitro* SPR: RBD binding of H11-H4 (K_D = 5 nM) and H11-D4 (K_D = 10 nM) ITC: RBD binding of H11-H4 (K_D = 12 nM) and H11-D4 (K_D = 39 nM) H11-H4 binds to the 'all down' and 'two down, one up' conformations of RBD The epitope on RBD that is recognized by H11-H4 slightly overlaps the ACE2 binding region RBD binding blocked by H11-H4-Fc (IC_{50} = 61 nM), H11-D4-Fc (IC_{50} = 161 nM) and VHH72-Fc (IC_{50} = 262 nM) *in vitro* ACE2 binding blocked by H11-H4-Fc (IC_{50} = 34 nM), H11-D4-Fc (IC_{50} = 28 nM) and VHH72-Fc (IC_{50} = 33 nM) *in vitro* *Inhibition of live virus* Nb-Fc neutralizes live virus H11-H4-Fc (ND_{50} = 6 nM) and H11-D4-Fc (ND_{50} = 18 nM)	September 2020 [84]

Table 3 (Continued)

Nbs and Nb constructs	Source	SARS-CoV-2 target	Nbs for neutralization and therapeutics	Date and reference
Ty1 Ty1-Fc	Alpaca immunization and phage display	SARS-CoV-2 protein	*Inhibition route* Ty1 specific and high affinity S RBD binding (K_D 5–10 nM) Bind RBD in the 'active' and 'inactive' state, thus blocking ACE2 binding Directly prevent RBD-ACE2 binding *Inhibition of pseudovirus* Neutralization of pseudotyped viruses (Ty1: IC_{50} = 0.77 µg/mL; Ty1-Fc: IC_{50} ~ 12 ng/mL)	September 2020 [86]
1E2 2F2 3F11 4D8 5F8	Synthetic phage display	S RBD	*Inhibition route* Prevent RBD and ACE2 binding/inhibit association K_D for the RBD protein against 1E2, 2F2, 3F11, 4D8, and 5F8 was 35.5, 5.1, 3.3, 6.0, and 0.9 nM, respectively 1E2 and 4D8 prevented RBD binding to ACE2 2F2, 3F11, and 5F8 partly compete for the RBD-ACE2 association *Inhibition of pseudovirus* Five sdAbs showed inhibition potency (EC_{50} = 0.0009–0.069 µg/mL) *Inhibition of live virus* The sdAbs showed neutralization efficiency (EC_{50} = 0.13–0.51 µg/mL) sdAbs and Fc fusions increase neutralization activity (EC_{50} = sub-nM level)	September 2020 [76]
2A 1B 3F VHH-Fc 3F-1B-2A	llama VHH (naïve and synthetic) libraries	S protein	*Inhibition route* Block SARS-CoV-2–ACE2 interaction Potent binding of S1 RBD VHH-Fc blocks S–ACE2 (K_D = 0.25 nM, IC_{100} ~36.7 nM, IC_{50} ~1 nM) 1B-3F VHH-Fc increased binding to S1 RBD and S–ACE2 blockade 3F-1B-2A VHH-Fcs (K_D ~ 0.047 nM) and 1B-3F-2A (K_D ~ 0.095 nM) bind S1 RBD more potently than VHH-Fc 1B-3F Tri-specific Nbs (3F-1B-2A [0.71 nM], 1B-3F-2A [0.74 nM]) blocked the S–ACE2 interaction more than mono-specific VHH-Fcs in combinations (IC_{50} = 2.21 nM) 3F-Fc and 2A-Fc likely bind to different S1 RBD epitopes 1B-Fc and 2A-Fc compete for binding to the same S1 RBD epitope 3F-Fc does not compete with 1B-Fc. *Inhibition of pseudovirus* Tri-specific VHH-Fcs (3F-1B-2A [IC_{50} = 3.00 nM] and 1B-3F-2A [IC_{50} = 6.44 nM]) neutralized pseudovirus infection more than the combination of VHH-Fcs (1B, 3F and 2A [IC_{50} = 29.19 nM])	October–December 2020 [85, 87]
Sb23 Sb23-Fc	Three Sb libraries	RBD	*Inhibition route* High RBD affinity (Sb23, K_D = 10 nM; and Sb23-Fc, K_D = 225 pM) Higher affinity for RBD than ACE2 Competes with ACE2 to bind RBD Competes with ACE2 for the same or overlapping binding sites on RBD Binds RBD in the 'up' and 'down' conformation Binds the inner edge of the ACE2 interaction interface of the RBD and inhibits ACE2 binding *Inhibition of pseudovirus* Pseudotyped virus neutralization (Sb23 [IC_{50} = 0.6 µg/mL] and enhanced by Sb23-Fc ~ 100-fold [IC_{50} = 0.007 µg/mL])	November 2020 [88]
Nb3 Nb6 Nb11 Nb6-tri mNb6 mNb6-tri	Yeast surface-displayed library of synthetic Nb sequences	S protein (mutant form)	*Inhibition route* Nb6 binds to S^{S2P} (K_D = 210nM) and RBD (K_D = 41 nM) Nb3 binds to S^{S2P} (K_D = 61 nM) but does not bind to RBD Nb6 (IC_{50} = 370 nM) and Nb11 (IC_{50} = 540 nM) potent inhibition of S^{S2P} binding to ACE2 Nb6 and Nb11 recognize RBD epitopes that overlap the ACE2 binding site Nb6 and Nb11 bind to open and closed S^{S2P} conformations Nb6 dimerization (750-fold) and trimerization (> 200,000-fold) increased K_D Disrupt S–ACE2 interaction *Inhibition of pseudovirus* Nb6 (IC_{50} = 2.0 µM), Nb11 (IC_{50} = 2.4 µM) and Nb3 (IC_{50} = 3.9 µM) inhibits pseudovirus infection Trimers enhance inhibition of pseudovirus Nb6-tri (2000-fold, IC_{50} = 1.2 nM) than Nb11-tri (40-fold, IC_{50} = 51 nM) and Nb3-tri (10-fold, IC_{50} = 400 nM) *Inhibition of live virus* Potent live virus neutralization by Nb6-tri (IC_{50} = 160 pM) and Nb3-tri (IC_{50} = 140 nM) *Inhibition route* mNb6-tri has a K_D of < 1 pM mNb-tri locks S into inactive format *Inhibition of pseudo and live virus* mNb6 elevated binding affinity (500-fold to S^{S2P}), pseudovirus and live virus inhibition (~ 200-fold) mNb6-tri increases inhibition of pseudovirus (IC_{50} = 120 pM or 5.0 ng/mL) and live virus (IC_{50} = 54 pM or 2.3 ng/mL) infection *Properties* mNb6-tri was stable and functional after heat exposure, lyophilization and aerosolization	December 2020 [11]

Table 3 (Continued)

Nbs and Nb constructs	Source	SARS-CoV-2 target	Nbs for neutralization and therapeutics	Date and reference
Nb21 Nb20 Nb89 $Nb21_3$ $Nb20_3$	llama immunization	S RBD	*Inhibition route* High affinities (Nb89 = 108 pM, and Nb20 = 10.4 pM) Epitopes of Nbs 20 and 21 overlap the hACE2 binding site Three copies of Nb20 or Nb21 simultaneously bind all RBDs in the 'down' conformations *Inhibition of pseudovirus* Pseudovirus neutralization (Nb89 [0.133 nM], Nb20 [0.102 nM], and Nb21 [0.045 nM]) *Inhibition of live virus* Live virus neutralization (Nb89 [0.154 nM], Nb20 [0.048 nM], and Nb21 [0.022 nM]) *Inhibition of pseudovirus* $Nb21_3$ and $Nb20_3$: pseudovirus inhibition increased ~ 30-fold ($Nb21_3$ [IC_{50} = 1.3 pM] and $Nb20_3$ [IC_{50} = 4.1 pM]) *Properties* Nb21 on-shelf stability after purification was ~ 6 weeks at room temperature Good solubility, thermostability (Nb89 = 65.9°, Nb20 = 71.8°, and Nb21 = 72.8°C) and high pseudovirus neutralization post lyophilization and aerosolization	Dec 2020 [89]
Nb91-hFc Nb3-hFc triNb91-hFc triNb3-hFc Nb91-Nb3-hFc	Naïve VHH library	S protein and RBD	*Inhibition route* Nb91-hFc binds the S and RBD protein Nb3-hFc recognizes the RBD protein *Inhibition of pseudovirus* Nb91-hFc (IC_{50} = 54.07 nM) and Nb3-hFc (IC_{50} = 32.36 nM) neutralize the pseudotyped virus Heterodimer Nb91-Nb3-hFc highest RBD binding affinity and pseudotyped virus neutralization (IC_{50} = 1.54 nM) Tri constructs enhanced RBD binding affinity and neutralizing ability triNb91-hFc (IC_{50}=4.89 nM) and triNb3-hFc (IC_{50}=4.70 nM) had enhanced pseudovirus neutralizing ability	January 2021 [105]
E, U, V, W, EE, EEE, Biparatopic Nbs VE, EV	Alpaca and llama immunization	S RBD	*Inhibition route* Target RBD and potent neutralization of infection E (K_D = 2 nM), U (K_D = 21 nM), V (K_D = 9 nM), and W (K_D = 22 nM) showed good RBD binding affinity VE (K_D = 84 pM) and EV (K_D = 200 pM) enhanced RBD binding E and U bind to distinct epitopes on the RBD E binds the ACE2 binding site on the RBD E binds 27 epitope residues, 16 of which are involved in ACE2 binding V binds a similar epitope as U and W, but in a different orientation on the RBD ACE2 binding was outcompeted by all Nbs dose-dependently E binds RBD in the three-up conformation Nbs trigger fusion machinery activation E, U, or W leads to cell-cell fusion V barely induced fusion EE and EEE did not induce fusion EV and VE induced fusion *Inhibition of pseudo and live virus* Good live virus-neutralizing activity (IC_{50} = 48–185 nM) EE and EEE: enhance neutralization of pseudotyped virus (EE: IC_{50} = 930 pM; and EEE: IC_{50} = 520 pM) and live wild-type virus (IC_{50} = 180–170 pM) VE and EV (IC_{50} = 4.1–2.9 nM) pseudotyped VSV neutralization Increased neutralizing activity of live wild-type (EV: IC_{50} = 0.7 nM; and VE: IC_{50} = 1.32 nM)	February 2021 [12]
W25 Monomeric W25FcM Dimeric W25Fc	Alpaca immunization	S protein	*Inhibition route* W25 RBD recognition and high-affinity binding (K_D = ± 295 pM) Efficiently competes with ACE2 for binding W25 (EC_{50} = 33 nM) RBD affinity is stronger than ACE2 *Neutralization of clinical isolates* Potent neutralization of wild-type and variants W25 potently neutralized D614 (IC_{50} = ± 9.82 nM) and G614 (IC_{50} = ± 5.09 nM) variants *in vitro* W25FcM neutralizes the D614 (IC_{50} = ± 27.40 nM) and G614 (IC_{50} = ± 12.36 nM) variants W25Fc neutralizes the D614 (IC_{50} = ± 7.39 nM) and G614 (IC_{50} = ± 3.69 nM)	February 2021 [106]

Table 3 (Continued)

Nbs and Nb constructs	Source	SARS-CoV-2 target	Nbs for neutralization and therapeutics	Date and reference
MR3 SR31 MR3-MR3 MR6-SR31 MR17-SR31	Sb libraries	S RBD	*Inhibition route and inhibition of pseudovirus* MR3: RBD binding (K_D = 1.0 nM), pseudovirus neutralization (IC_{50} = 0.40 μg mL^{-1}) and competes with ACE2 to bind RBD MR6 (K_D = 23.2 nM and IC_{50} = 77.5 nM) MR17 (K_D = 83.7 nM and IC_{50} = 747 nM) MR3 and MR17 targets RBD at the RBM surface and blocks the ACE2–RBD interaction MR3-MR3 neutralization activity (IC_{50} = 10 ng mL^{-1}) MR3-MR3 inhibit pseudotypes with the original S or mutant D614G S *Inhibition of in vivo infection* MR3-MR3-ABD (25 mg kg^{-1} intraperitoneal) provides prophylactic protection against infection in hamsters *Inhibition route and inhibition of pseudovirus* SR31: highly binds RBD (K_D = 5.6 nM) but no neutralization. Fusion partner potential SR31-binding epitope is distant from the RBM Binding of SR31 does not cause steric hindrance for ACE2-binding SR31 does not compete with MR17 and MR6 Conjugates: elevated RBD affinity (MR17-SR31 [K_D = 0.3 nM] and MR6-SR31 [K_D = 0.5 nM]) and pseudovirus neutralization (MR17-SR31 [IC_{50} = 52.8 nM] and MR6-SR31 [IC_{50} = 2.7 nM])	June 2020–March 2021 [90, 91]
Nb4-43, Nb11-59, Nb14-33, Nb15-61, Nb16-52, Nb16-68, HuNb11-59	Camel immunization and phage display	S RBD	*Inhibition route* High-affinity RBD binding (K_d = 21.6–106 nM) The EC_{50} and IC_{50} values are lower than 0.2 and 1 μg/mL, respectively Varying levels of RBD–ACE2 blocking activity (Nb8-87 [16.2%], Nb13-58 [50.4%], and Nb11-59 [98.9%]) Binding capacity to wild-type and mutant RBD Blocks RBD–ACE2 interaction Binding to eight S RBD mutants (Q321L, V341I, N354D, V367F, K378R, V483A, Y508H, and H519P variants) and block their interaction with ACE2 *Inhibition of live virus* Potent activity against authentic virus (Nb16-68 [ND_{50} = 2.2 μg/mL] and Nb11-59 [ND_{50} = 0.55 μg/mL]) *Properties* Large-scale production of HuNb11-59 in *Pichia pastoris* (20 g/L titer and 99.36% purity) HuNb11-59: elevated purity, stability (4 or 25°C for up to 4 weeks) and neutralization activity Stable after nebulization and inhale delivery potential	March 2021 [92]
PiN-21	Llama immunization	S RBD	Prevents infection *in vitro* *Inhibition of in vivo infection* Viral replication inhibited by intranasal (0.6 mg/kg) delivery *in vivo* Viral load decreased, pneumonia and lung damage prevented by aerosol (~ 0.2 mg/kg) delivery *in vivo*	May 2021 [5]
WNb 2 WNb 7 WNb 15 WNb 36 WNbFc 2 WNbFc 7 WNbFc 15 WNbFc 36	Alpaca immunization	S protein and RBD	*Inhibition route* High affinities (K_D = 0.14–19.49 nM) Neutralizing activity (3–36 nM) Potently abolished RBD-ACE2 complex formation Binding of WNb 2 and WNb 10 overlaps the ACE2 binding site on the RBD WNbFc fusions bind to distinct antigenic sites on RBD (nM), inhibit ACE2/RBD complex formation WNbFc bind with low nM affinity to RBD and with pM affinity to S WNbFc bind to most RBD variants (EC_{50} = 0.7–14 nM) WNbFc binds to wild-type RBD (EC_{50} = 0.97–2.65 nM) but decreased binding to either E484K or N501Y variant RBDs WNbFc fusions binding to wild-type RBD and N501Y variant (K_D < 0.55 nM) WNbFc (IC_{50} = 0.16–0.61 nM) inhibits wild-type RBD–ACE2 engagement and most RBD variants (IC_{50} = 0.04–1.8 nM) WNbFc fusions block ACE2 interaction with the E484K variant to a greater extent (IC_{50} = 0.04–0.19 nM) *Inhibition of live virus* WNbFc (IC_{50} = 0.10–3.18 nM) neutralizes wild-type WNbFc (IC_{50} = 0.11–5.04 nM) neutralizes N501Y D614G Disrupt the RBD–ACE2 interaction Virus neutralization Nb-Fc: Inhibits ACE2 and variant RBD interaction Potent wild-type and variant neutralization *Inhibition of in vivo infection* Prophylactic Nb-Fc (5 mg/kg, intraperitoneal injection) administration reduced variant viral loads *in vivo* against a human clinical isolate of SARS-CoV-2 (hCoV-19/Australia/VIC2089/2020), which has the N501Y D614G mutations	May 2021 [17]

Table 3 (Continued)

Nbs and Nb constructs	Source	SARS-CoV-2 target	Nbs for neutralization and therapeutics	Date and reference
aRBD-2 aRBD-3 aRBD-5 aRBD-7 aRBD-41 aRBD-54 aRBD-2-5 aRBD-2-7	Alpaca immunization and phage display	RBD	*Inhibition route* Bind RBD and S1 domain High-affinity RBD binding (K_D = 2.60–21.9 nM) N501Y variant did not affect binding to the seven Nbs Nb-Fc fusions increased binding capability (K_D = 1.59–72.7 pM) Nbs and their Fc fusions effectively blocked ACE2/RBD binding dose-dependently Nb-Fc fusions enhance blocking activities (5- to 90-fold decrease in IC_{50}) Nb-Fc fusions inhibit ACE2-Fc binding (10 nM) to RBD with IC_{50} values at the nM level The hetero-bivalent Nbs (aRBD-2-5 [K_D = 59.2 pM] and aRBD-2-7 [K_D = 0.25 nM]) and their Fc fusions (K_D = 12.3 pM and K_D = 0.22 nM) enhance binding affinities *Inhibition of live virus* The aRBD-2, aRBD-5, and aRBD-7 modestly neutralize live virus (33–100 µg/mL) The aRBD-2-Fc (ND_{50} = 0.092 µg/mL), aRBD-5-Fc (ND_{50} = 0.440 µg/mL), and aRBD-7-Fc (ND_{50} = 0.671 µg/mL) showed enhanced neutralization potency *Properties* High stability	May 2021 [107]
Nb15 Nb17 Nb19 Nb56 Nb12 Nb30	Llama immunization Nanomice immunization	RBD and S protein	*Inhibition route* High binding affinity of (K_D < 30 nM) Nb15 and Nb56 inhibit ACE2-S protein binding Nb12 induces a 'two up and one down' S conformation Nb12 recognizes a region in the middle of the RBD, outside the ACE2-binding region Nb30 to induce a 'three up' conformation Nb17, Nb19 and Nb56 inducing a 'one up' conformation Nb15 associates with 'all down' conformation *Inhibition of pseudo and live virus* Pseudotyped virus neutralization ranged from Nb12 (IC_{50} = 11.7 nM) to Nb19 (IC_{50} = 0.335 nM) Nb15 ineffective against N501Y Nb17, Nb19 and Nb56 ineffective against E484K alone or E484K with K417N and N501Y Bivalent or trivalent forms (Nb15, Nb19 and Nb56) potently bind and neutralize Nb15 and Nb56 trimers (IC_{50} = 14–30 pM) Nb12 and Nb30 neutralization potency mostly unaffected by RBD mutations Trivalent (Nb15, Nb56 and Nb12) and bivalent (Nb30) Nbs neutralized authentic virus of wild-type, the B1.1.7, B1.351 and P.1 variants Most effective against the B1.1.7 variant (IC_{50} = 4–538 pM) and less effective against the B.1.351 variant (IC_{50} = 18–2755 pM)	June 2021 [108]
SR4 MR3 MR4 MR17 LR1 LR5 MR3-MR3 MR3-MR3-ABD	Sb libraries	S RBD	*Inhibition route and inhibition of pseudovirus* High-affinity RBD binding K_D ranging from 83.7 nM (MR17) to 1.0 nM (MR3) Neutralization by blockage of the ACE2–RBD interaction competitively MR3, SR4 and MR17 target RBD at the RBM surface MR3: high RBD binding affinity (K_D = 1.0 nM) and pseudovirus neutralization activity (IC_{50} = 0.42 µg mL^{-1}) MR17 binding (K_D = 83.7 nM) LR5-MR3 was more potent (IC_{50} = 0.11 µg mL^{-1}) Decreased IC_{50} by Fc fusion: Fc-MR3 (10-fold, 42 ng mL^{-1}) and Fc-MR17 (27-fold, 0.46 µg mL^{-1}) Increased K_D by Fc fusion: Fc-MR3 (0.22 nM) and Fc-MR17 (< 1 pM) MR3-MR3 increased neutralization activity (40-fold, IC_{50} = 10 ng mL^{-1}) MR3-MR3 inhibit pseudotypes of the original S and mutant D614G *In vivo*, MR3-MR3-ABD bind RBD and neutralize pseudotypes with 614D and 614G S *Inhibition of in vivo infection* Sbs showed prophylactic protection from infection *in vivo* In hamsters, divalent sybodies (2.5 mg) administered intraperitoneally before infection with SARS-CoV-2 (strain BetaCoV/Munich/BavPat1/2020), MR3-MR3-ABD decreased viral RNA load in the lung (7-fold) but not in nasal turbinates *In vitro*, MR3-MR3-ABD and Fc-MR3 had similar potency; however, in hamsters, MR3-MR3-ABD was less effective than Fc-MR3	July 2021 [98]

Table 3 (Continued)

Nbs and Nb constructs	Source	SARS-CoV-2 target	Nbs for neutralization and therapeutics	Date and reference
Tetravalent VHH-72 Hexavalent VHH-72	–	–	*Inhibition route* VHH-72 high-binding affinity (K_D = 29–60 nM) for wild-type and variants (UK and SA) ACE2 competes with VHH-72 for RBD binding *Inhibition of pseudovirus* Increased wild-type neutralization potency of bivalent VHH-72 (IC_{50} = ± 3.3 nM), tetravalent (IC_{50} = ± 0.34 nM) and hexavalent (IC_{50} = ± 0.03 nM) Substantial synergistic increases in neutralization efficacy Hexavalent Nb: potent pseudovirus neutralization of the UK (IC_{50} = ± 0.31 nM) and SA (IC_{50} = ± 0.07 nM) variants *Properties* Multivalent Nbs: high stability and solubility	August 2021 [14]
Nb-Fc constructs: SP1B4 SP1D9 SP3H4	Synthetic highly diverse Nb phage library	S protein and RBD	*Inhibition of pseudovirus* Potent pseudovirus and wild-type neutralization SP1B4 (EC_{50} = 0.33 nM), SP1D9 (EC_{50} = 0.45 nM) and SP3H4 (EC_{50} = 0.14 nM) showed strong neutralization of VSV-SARS-CoV-2-GFP SP1B4 (EC_{50} = 3.14), SP1D9 (EC_{50} = 1.12) and SP3H4 (EC_{50} = 0.70 nM) showed strong neutralization of wild-type *Inhibition route* SP1B4 (K_D = 39.5 nM) and SP1D9 (K_D = 8.9 nM) high affinity for RBD SP1B4 (K_D = 97.7 nM) and SP1D9 (K_D = 49.7 nM) affinity for the Alpha RBD Beta variant no detectable binding for SP1B4, SP1D9 or SP3H4 *Inhibition of in vivo infection* SP1D9 and SP3H4: prophylactic and therapeutic (intraperitoneal injection, 10 mg/kg) efficacy against fully virulent wild-type *in vivo*	August 2021 [9]
Nanosota-1A *Nanosota-1B* *Nanosota-1C* *Nanosota-1C-Fc*	Naive camelid Nb phage display library	RBD	*Inhibition route* *Nanosota-1A, -1B, and -1C* bind RBD with increasing affinity (K_d = 228–14 nM) *Nanosota-1C-Fc* binds RBD with the highest affinity (K_d = 15.7 pM) and ~ 3000 times tighter than ACE2 *Nanosota-1C* binds close to the center of the SARS-CoV-2 RBM 14 RBM residues directly interact with *Nanosota-1C*, and 6 of these also directly interact with ACE2 *Nanosota-1C* accesses open and closed conformations of the S protein *Inhibition of pseudovirus* *Nanosota-1C* and *Nanosota-1C-Fc* compete with ACE2 and inhibit pseudovirus and live virus *in vitro* *Nanosota-1C-Fc* potent pseudovirus neutralization (ND_{50} = 0.27 µg/mL and ND_{90} = 3.12 µg/mL) which was ~ 10 times greater than *Nanosota-1C* and ~ 160 times greater than ACE2 *Nanosota-1* strongly neutralizes pseudovirus bearing the D614G mutation *Inhibition of live virus* *Nanosota-1C-Fc* potently neutralizes live virus infection (ND_{50} = 0.16 µg/mL) to a greater extent than *Nanosota-1C* and ACE2 *Inhibition of in vivo infection* *Nanosota-1C-Fc* preventive and therapeutic (intraperitoneal, 10–20 mg/kg) efficacy against live infection (culture infectious dose) *in vivo* *Properties* Thermostable (− 80 °C, 4 °C, 25 °C, or 37°C for 1 week) *In vivo* stability (10 days) Biodistribution (3 days)	August 2021 [48]
> 800 predicted Nb binder families SR38 Affinity maturation SR6v1 SR6v7 SR6v9 SR6v15	Cell-free VHH identification using clustering analysis (CeVICA)	S protein RBD domain	*Inhibition route and inhibition of pseudovirus* Developed CeVICA Produced 30 true binders and 11 neutralizers of pseudotyped virus SR38 binds RBD with N501Y mutation and neutralization of N501Y pseudovirus SR6v15—highest binding (K_D = 2.18 nM) Produced a dimer (SR6v15.d) and trimer (SR6v15.t) High pseudovirus neutralization of SR6v15.d (IC_{50} = 0.329 nM) *Properties* Thermal stability	September 2021 [109]

Table 3 (Continued)

Nbs and Nb constructs	Source	SARS-CoV-2 target	Nbs for neutralization and therapeutics	Date and reference
C5 H3 C1 F2 C5-Fc Trimeric C5	llama immunization	RBD and S protein	*Inhibition route* High binding affinity of H3, F2, C5, and C1 (K_D = 20–615 pM). C1, H3 and C5 blocked ACE2 binding, whereas F2 did not affect ACE2 binding Bind to different strains For RBD binding, C1 and F2 competed with CR3022, whereas C5 and H3 competed with H11-H4 C5 binds to RBD (K_D = ± 210 pM) and S (K_D = ± 350 pM) with high affinity C5 and H3 strongly binds the Alpha variant but not the Beta strain C1 and F2 binds the wild-type, Alpha, and Beta variants at similar affinities Trimeric (C5, C1 and H3) Nbs bind to RBD at an enhanced K_D (10- to 100-fold) Trimers neutralize/block Victoria, Alpha or Beta strains/infection C5-Fc: high RBD binding affinity (K_D = 37 pM) *Inhibition of pseudo and live virus* The C5 neutralizes the Victoria (IC_{50} = 18 pM) and Alpha (IC_{50} = 25 pM) strains C1 was active against the Beta strain High neutralization potency of C5 trimer against the live Victoria strain (ND_{50} = 3 pM) C5-Fc: high virus neutralization potency (ND_{50} = 2 pM) *Inhibition of in vivo infection* Therapeutic efficacy against the Victoria strain by intraperitoneal C5-Fc (4 mg/kg) administration *in vivo* Therapeutic benefit by intraperitoneal and intranasal trimeric C5 (4 mg/kg) administration *in vivo*	September 2021 [93]
Nb_{15}-Fc Nb_{22}-Fc Nb_{31}-Fc Nb_{15}-Nb_H-Nb_{15}	Alpaca immunization and phage display	Extracellular domain of S protein	*Inhibition route* Specific RBD binding of 14 Nb-Fcs (K_D = 4.25–37.6 nM) Tightly clustered RBD binding of Nb_{15}-Fc, Nb_{22}-Fc, and Nb_{31}-Fc (K_D = 1.13–1.76 nM) Nb_{15}-Fc, Nb_{22}-Fc, and Nb_{31}-Fc recognize overlapping epitope on RBD with nM affinities *Inhibition of pseudo and live virus* Potent neutralization of pseudotyped, live virus and variants Nb_{15}-Fc, Nb_{22}-Fc and Nb_{31}-Fc showed potent neutralization of live virus (IC_{50} = 41.3–75 pM and IC_{90} = 195–293.8 pM) and pseudovirus (IC_{50} = 10–28.8 pM) Did not inhibit MERS-CoV or SARS-CoV pseudovirus Inhibited 15 SARS-CoV-2 variants Inhibited the replication of SARS-CoV-2 variants with a D614G mutation Nb_{15}-Fc: highest neutralization potency The bivalent Nb_{15} (IC_{50} = 11 pM), trivalent Nb_{15} (IC_{50} = 9.0 pM), and tetravalent Nb_{15} (IC_{50} =4.3 pM) showed enhanced neutralization potency compared with monomeric Nb_{15} (IC_{50} = 2.3 nM) Increasing K_D (12 to < 0.001 nM) as the valence increased Nb_{15}-Nb_H-Nb_{15}: enhanced neutralization of wild-type and variants *in vitro* Specific RBD (K_D = 0.54 nM) and HSA (K_D = 7.7 nM) binding pM potency against the wild-type and 18 mutant variants Potency against the pseudotyped variants with D614G and N501Y mutations (UK and SA) Potent neutralization against pseudotyped variants wild-type (IC_{50} = 9.0pM), Alpha (IC_{50} = 5.9pM) and Delta (IC_{50} =116 pM) Failed to neutralize Gamma and Beta *Properties* Excellent thermal stability 70–80 °C 1 h *Inhibition of in vivo infection* Favorable (average of 10 mg/kg) intranasal administration led to prophylactic and therapeutic efficacy *in vivo* (Strain IVCAS 6.7512)	October 2021 [74]

Table 3 (Continued)

Nbs and Nb constructs	Source	SARS-CoV-2 target	Nbs for neutralization and therapeutics	Date and reference
Re6B06 Re9F06 Re5D06 Re9B09 Re6H06 Re5F10 Re9H01 Re9H03 Re6B07	Alpaca immunization and phage display	SARS-CoV-2 complete S1 fragment and the RBD	*Inhibition route and neutralization* SARS-CoV-2 neutralization, tight RBD binding, bind the S protein in the open and closed states Re6B06 and Re9F06 bind RBD (K_D = 4–12 nM) Tight RBD-binding of Re5D06 (K_D ~2 pM), Re9B09 (K_D ≤1 pM), Re6H06 (K_D ≤1 pM), Re5F10 (~30 pM), Re9H01 (~10 pM), and Re9H03 (~25 pM) Low nM-range neutralization (Re9F06 [17 nM], Re5F10 [5 nM], Re6B07 [5 nM], and Re6B06 [50 nM]) pM-range neutralization (Re9B09, Re9H01, Re9H03 [167 pM], Re5D06 and Re6H06 [50 pM]) Re5D06, Re6H06 or Re9B09 block the ACE–RBD interaction Re5F10, Re7E02 or Re9F06 also competed with ACE2 The trimerization of Nbs decreased the minimal neutralization concentration (Re9F06 =167 pM, Re6D06 = 17 pM) Re5D06–RBD model can accommodate the N501Y exchange Combination of mutations Beta (K417N, E484K, N501Y) or Gamma (K417T, E484K, N501Y) decreased Re5D06–RBD interaction (K_D = 0.1–0.5 nM) Produced a tandem by fusion of Re9F06 to R28 Tandem binds rapidly to the Beta and Gamma variants Produced a quadruple (K417T, L452R, E484K, N501Y) RBD mutant Re9F06-R28 tandem binds the mutant Re6H06 ≤10 pM binding to either the Beta or Gamma variants Re9H03 binds mostly irreversibly to Gamma, Beta and the quadruple mutant Potent B.1.351 neutralization by monomers (Re5F10 [1.7 nM], Re6H06 [170 pM], Re9B09 [1.7 nM], Re9H03 [50–170 pM]) and tandems (Re9F06-R28 [50 pM], Re9F06-Re9B09 [50 pM], and Re9F06-Re6H06 [17 pM]) *Properties* Re9B09, Re5D06, Re9F06 and Re5F10 are hyperthermostable (90°C, 5 min) or can robustly refold after heat treatment	October 2021 [4]
K-874A	An extensive DNA library	S protein S1 domain	*Inhibition route* Strong and specific S1 affinity (K_d = 1.4 nM) but not to other coronaviruses (HCoV and SARS-CoV-1) Inhibits SARS-CoV-2 infection (IC_{50} = ± 5.74 µg/mL) Does not prevent virus attachment to host the ACE2 receptor Prevents virus entry by blocking viral fusion to the host cell K-874A neutralizes through a different route that does not involve ACE2 binding Neutralizes only the B.1.1.7 variant *Inhibition of in vivo infection* K-874A (30 mg/kg) administered intranasally, decreased virus levels in the lungs and inhibits cytokine induction *in vivo*	October 2021 [94]
NIH-CoVnb-112	llama immunization and phage display	S protein RBD	*Inhibition route and inhibition of pseudovirus* Low K_D for prototype RBD (1.59 nM), Alpha (3.0 nM), Beta (4.28 nM), Gamma (4.16 nM) and Delta (1.66 nM) High RBD binding affinity (4.9 nM) and interferes with RBD–ACE2 interaction (EC_{50} = 0.02 µg/mL) Highly binds to variants (N354D, D364Y, V367F, and W436R) and blocks the variants–ACE2 interaction Blocks pseudotyped virus infection *in vitro* Variant pseudovirus neutralization of Alpha (EC_{50} = 9.4 nM), Beta (EC_{50} = 15.8 nM), Gamma (EC_{50} = 17.6 nM), and Delta (EC_{50} = 14.5 nM) *in vitro* *Properties* Maintains effectiveness post-nebulization The pre-nebulization and post-nebulization samples incubated (37°C for 24 h) appeared the same with no indication of degradation/aggregation products Stable at physiological temperature Nebulized delivery decreased viral burden and lung pathology *in vivo* *Inhibition of in vivo infection* Initial *in vivo* protective efficacy (nebulization, 25 mg/mL) against prototype SARS-CoV-2	December 2020–March 2022 [95, 96]

Table 3 (Continued)

Nbs and Nb constructs	Source	SARS-CoV-2 target	Nbs for neutralization and therapeutics	Date and reference
Fu2 Fu2-Fc Fu2 homodimer Fu2-Ty1 Fu2-Alb1	Alpaca immunization	S protein and RBD	*Inhibition route and Inhibition of pseudovirus* Potent pseudovirus neutralization and greater potency than Ty1 High RBD binding affinity (nM) Fu2 prevents S–ACE2 binding, blocks RBD–ACE2 binding, binds RBD in the 'up' conformation and neutralizes variants Fu2 (IC_{50} = 7 nM) potent neutralization of pseudotyped virus (~ 10 times than Ty1) The Fu2-Fc and Fu2 homodimer (IC_{50} = 0.75–0.8 nM) neutralized pseudotyped virus The Fu2-Ty1 (IC_{50} = 140 pM) potently neutralized pseudotyped virus Fu2 neutralizes pseudotyped Beta and Delta variant at similar potency *Inhibition of live virus* Fu2, dimeric Fu2 and Fu2-Ty1 neutralizes live (SARS-CoV-2 and Beta variant) virus with increasing potency Fu2 and Fu2 dimeric constructs neutralize SARS-CoV-2 (N_{50} = Fu2 [6.1 µg/mL], Fu2-Fc [570 ng/mL] and Fu2 dimer [57 ng/mL]) *Inhibition of in vivo infection* In K18-hACE2 transgenic mice (SARS-CoV-2 and beta variant), Fu2-Alb1 (intraperitoneal injection, 600 µg/day, 1–6 days) decreased viral loads and delayed onset of disease *in vivo*	January 2022 [99]
Nb1 Nb2 Nb15 Biparatopic Nb: Nb1–Nb2 Nb1–Nb2-Fc	Synthetic Nb phage display library	RBD proteins	*Inhibition route and inhibition of pseudovirus* Nb1, Nb2 and Nb15 (0.33 µM) neutralized S pseudotyped variants (B.1.1.7, B.1.341, P.1 and B.1.617) Nb1 binds wild-type, Alpha, Beta, Gamma and Delta variants RBDs (K_D = 4.4 to < 0.001 nM) Nb2 binds wild-type, Alpha and Delta RBDs (K_D = 7.8–0.37 nM) Nb1–Nb2: High affinity and neutralization of variants Strong escape-resistant feature Potent neutralizer of the Delta variant pseudovirus (IC_{50} = 0.0036 nM) High affinity (K_D < 0.001 nM) to RBDs of the wild-type, Alpha, Beta, Gamma and Delta variants Neutralizes variant (Alpha, Beta, Gamma and Delta) pseudoviruses (IC_{50} = 0.003–0.0865 nM) *Inhibition of live virus* Neutralizes live (SARS-CoV-2 GFP/ΔN trVLP) wild-type virus (IC_{50} = 1.207 nM) and variant virus (Alpha, Beta, Gamma and Delta [IC_{50} = 0.8149–13.01 nM]) Nb1–Nb2-Fc: Improved neutralization activity, yield and stability Strongest affinity ($K_D < 1.0 \times 10^{-12}$ M) Extremely potent neutralization against variants of concern (IC_{50} = 0.0097–0.0987 nM) Potently neutralized Omicron pseudovirus (IC_{50} = 0.0017 nM) and live virus (IC_{50} = 1.46 nM)	February 2022 [110]
c19s130Fc (gp130 and VHH72)	–	–	Blocks both IL-6 *trans*-signaling and viral infection c19s130Fc showed high affinity (55pM) for hyper-IL-6 *Inhibition route* c19s130Fc (IC_{50} = 1 nM) c19s130Fc binding affinity for S-RBD (880 nM) c19s130Fc (78 nM) decreased S-RBD/ACE2 interaction by 40% c19s130Fc decreased virus cell entry (IC_{50} = ± 15.1 nM)	February 2022 [111]
Biparatopic Nbs NM1267 NM1268	Alpaca immunization	RBD	*Inhibition route and neutralizations* NM1267: binding affinities to variants (Alpha, Beta, Gamma and Delta [K_D = 55.8 – 764.4 pM]) NM1267 (IC_{50} ~ 0.9 nM) showed increased neutralization NM1267, we observed a strong neutralization B.1 (IC_{50} = 0.33 nM), B.1.351 (IC_{50} = 0.78 nM) and B.1.617.2 (IC_{50} = 52.55 nM) Targets different RBD epitopes NM1268: strong binding affinities to variants (Alpha, Beta, Gamma and Delta [K_D = < 1.6–114 pM]) NM1268: strong neutralization potency for B.1 (IC_{50} = 2.37 nM), B.1.351 (IC_{50} = 6.06 nM), and B.1.617.2 (IC_{50} = 0.67 nM) *Inhibition of in vivo infection* Prophylactic intranasal NM1267 treatment (20 µg) blocks variant (B.1 infection)-induced disease and mortality *in vivo* In mice, NM1267 reduced signs of disease and virus shedding Prophylactic NM1267 treatment decreased lung tissue damage induced by virus and inflammation in B.1-infected mice Prophylactic NM1267 treatment blocked disease progression in B.1.351 variant-infected mice NM1267 and NM1268 prevents disease progression and mortality due to B.1, B.1.351 and B.1.617.2 infection *Properties* High stability, purity and production yields	February 2022 [77, 78]

Table 3 (Continued)

Nbs and Nb constructs	Source	SARS-CoV-2 target	Nbs for neutralization and therapeutics	Date and reference
ABS-VIR-001 (1B-3F-2A-Fc)	–	–	*Inhibition route and inhibition of in vivo infection* Intranasal (10 mg/kg) prophylaxis prevents viral infection and death *in vivo* Post-exposure treatment decreases viral loads Binds and blocks ACE2 interaction of wild-type S RBD and tri-mutant S RBD (K417N, E484K and N501Y) Efficacy at decreasing variant (Alpha, Beta, Delta and Omicron) S–ACE2 interaction 10 mg/kg prevents pseudovirus infection (SARS-CoV-2-luc pseudovirus via the intranasal route) *in vivo* 25 mg/kg prevents authentic virus infection and decreases viral load *in vivo* Effective (intranasal and intraperitoneal) as a prophylaxis treatment and a treatment for SARS-CoV-2 Strong binding of the Tri-mutant (K_D = 2.49E-10 M) *Properties* High thermostability (stable after 4 weeks at 45°C)	March 2022 [100]
P2C5 P2G1 P5F8 P2C5-P5F8	Bactrian camel immunization	RBD	*Inhibition route and inhibition of live virus* High neutralization potency High-affinity RBD binding by P2C5 (K_D = 3.97 nM), P2G1 (K_D = 5.36 nM) and P5F8 (K_D = 1.94 nM) Neutralization of live virus by P2C5 (EC_{50} = 3.35 nM), P2G1 (EC_{50} = 21.39 nM) and P5F8 (EC_{50} = 11.73 nM) *in vitro* P2C5 blocks ACE2–RBD interaction (90% at 0.5 µg/mL) P2C5 monomer neutralized Alpha, Beta, Gamma and Omicron, but not Delta P5F8 and P2G1 monomer all variants of concern except Omicron P2C5-P5F8 highly neutralizes the Alpha, Beta, Gamma, Delta and Omicron variants (89 pM, 356 pM, 356 pM, 2.85 nM and 709 pM, respectively) P2C5-P5F8 heterodimer increased (100 times) neutralization activity (178 pM)	February 2022 [112]
saRBD-1 Fc-saRBD-1 BisaRBD-1	Alpaca immunization	S RBD	*Inhibition route* High-affinity binding saRBD-1: Binds to full-length trimer (EC_{50} = 100 pM), S1 (EC_{50} = 200 pM) and to RBD (EC_{50} = 607 pM) Binds to RBD (K_D = 750 pM), S1 (K_D = 1880 pM) and S trimer (K_D = 674 pM) Disrupt the RBD–ACE2 interaction by competitive binding to the S RBD saRBD-1 binds competitively with ACE2 saRBD-1 (6 nM) blocks 50% of ACE2 binding Completely blocks infection (179 nM) *Inhibition of pseudo and live virus* Neutralizes pseudotyped (GFP-bearing SARS-CoV-2 S) virus (IC_{50} = 4.26 nM) and live (SARS-CoV-2 WA1/2020 strain) virus ($FRNT_{50}$ = 7.4–5.82 nM) Neutralizes variants (Alpha, Beta, Gamma, Delta [$FRNT_{50}$ = 15.84–19.95 nM]) Fc-saRBD-1 and BisaRBD-1: Improved binding and neutralization Fc-saRBD-1 has stronger affinity (EC_{50} = 392 pM, and K_D = 302 pM) Fc-saRBD-1 improved pseudovirus neutralization (IC_{50} = 100 pM) and live virus ($FRNT_{50}$ = 118–218 pM) BisaRBD-1 live virus neutralization ($FRNT_{50}$ = 243–728 pM) Fc-saRBD-1 ($FRNT_{50}$ = 76–387 pM) and Bi-saRBD-1 ($FRNT_{50}$ = 56–235 pM) potently neutralizes variants (Alpha, Beta, Gamma, Delta) *Properties* Stable and active after heat treatment, lyophilization and nebulization ($FRNT_{50}$ = 3.00–9.01 nM)	March 2022 [113]
Sb#15 Sb#68 GS4 Tripod-GS4r	Synthetic library	RBD	*Inhibition route* Sb#15 and Sb#68 simultaneously bind S protein with high affinity (9–12 nM) Sb#15 and Sb#68 compete/block ACE2 binding to S Sb#15 binding epitope strongly overlaps with the ACE2 binding site Sb#68 recognizes a conserved 'cryptic' epitope that is distinct from the ACE2 interaction site *Inhibition of pseudo and live virus* Effective neutralization of pseudoviruses Sb#15 (IC_{50} = 147 nM) and Sb#68 (IC_{50} = 138 nM) Sb-Fc constructs neutralize pseudoviruses (Sb#15 [IC_{50} = 16 nM] and Sb#68 [IC_{50} = 50 nM]) Neutralization of live virus by Sb#15 (ND_{50} = 561 nM) and Sb#68 (ND_{50} = 377 nM) Sb#15 and Sb#68 were fused resulting in GS4 GS4 increased S binding affinity ($K_d \approx 0.3$ nM) and neutralization potency (pseudotyped [IC_{50} = 0.7 nM] and live [ND_{50} = 2.6 nM] virus) GS4 no escape mutants Tripod-GS4r: greater neutralization potency (low pM)	April 2022 [114]

Table 3 (Continued)

Nbs and Nb constructs	Source	SARS-CoV-2 target	Nbs for neutralization and therapeutics	Date and reference
7A3 8A4 1B5 8A2 2F7 1H6	Dromedary camels by phage display	RBD and the S trimer	*Inhibition route* High binding affinity for wild-type and variants All V_HH-hFc showed binding affinity (nM) to the Wuhan-Hu-1 and B.1.1.7 variants 8A2, 7A3 and 1B5 (0.001–0.8 nM) strong S binding for the B.1.351 and P.1 variants 7A3 (K_D =0.96 nM), 8A2 (K_D =0.8 nM), and 2F7 (K_D =0.75 nM) Bind two distinct epitopes on the RBD with high affinity 8A2 disrupts the ACE2 binding, 7A3 binds a unique site that involves the residues of the S2 subunit 7A3 binds the 'up and down' conformation Only 1B5 (0.14 nM) and 7A3 (0.42 nM) bound to B.1.617.2 Best ACE2 blockers were 1B5 (IC_{50} = 3.2 nM) and 8A2 (IC_{50} = 8 nM) *Inhibition of pseudo and live virus* 8A2 most potent pseudovirus neutralizer (IC_{50} = 5 nM) and virus with or without D614G 7A3 + 8A2 (IC_{50} = 1.6 nM) most effective against pseudovirus 7A3 + 8A2 (IC_{50} = 0.2–1 nM) most effective neutralizer of the original virus and variants (B.1.1.7, B.1.351, and P.1) 7A3 + 8A2 potent activity against live virus wild-type strain (IC_{50} = 20 nM) and variants (D614G, B.1.1.7, B.1.351, P.1 and B.1.617.2 [IC_{50} 0.14 – 27 nM]) *Inhibition of in vivo infection* In K18-hACE2 mice, 7A3 V_HH-hFc or 7A3+8A2 (intraperitoneal, 5 mg/kg) protects against lethal B.1.351 infection Protective efficiency of 7A3+8A2 (intraperitoneal, 5 mg/kg) was decreased (50%) by exposure to a lethal dose of B.1.617.2	May 2022 [97]
Nb-007 Nb-007-Fc	Alpaca immunization	S RBD	*Inhibition route and Inhibition of pseudovirus* Nb-007 binds S-RBD (K_D = 67.4 pM) with higher affinity than ACE2 and virus entry-inhibition activity Competitively binds RBD Neutralization activity against pseudotyped virus and Delta variant Nb-007 inhibits pseudovirus infection (IC_{50} = 37.6 nM) 126 nM in the cell-cell fusion inhibition assay Nb-007 directly competes with ACE2 Nb-007 had decreased S-RBD binding affinity to variants (Beta [K_D = 1.75 μM] and Delta [K_D = 109 nM]) and neutralization of pseudotyped variant viruses (Beta [IC_{50} = 8.13 μM] and Delta [IC_{50} =1.07 μM]) Nb-007-Fc increased binding affinity of variants (Beta [K_D = 44.4 nM] and Delta [K_D = 0.929 nM]) and neutralization of pseudotyped viruses (wild-type [IC_{50} = 1.64 nM], Beta [IC_{50} = 405 nM] and Delta [IC_{50} = 42.6 nM]) Nb-007-Fc showed increased virus entry-inhibition activity	May 2022 [115]
DL4	Alpaca immunization	RBD	*Inhibition route and inhibition of pseudovirus* High RBD affinity (K_D = 0.25 nM) Competitively binds RBD Directly competes with ACE2 Neutralization of pseudoviruses Wuhan strain and Alpha strain (IC_{50} = 6.23 nM) Neutralizes by directly blocking the receptor recognition	June 2022 [116]
DL28	Alpaca immunization	RBD	*Inhibition route and Inhibition of pseudovirus* Tight RBD binding (K_D = 1.56 nM) Blocks ACE2 binding DL28 neutralizes wild-type (IC_{50} = 5.39 nM) and variants (Alpha [IC_{50} = 4.61 nM], Beta [IC_{50} = 13.95 nM], Gamma [IC_{50} = 17.16 nM], Delta [IC_{50} = 21.88 nM] and Omicron [IC_{50} = 8.68 nM]) pseudoviruses	Jun 2022 [117]
RBD-1-2G RBD-1-2G-Fc RBD-1-2G-Tri	Humanized Nb library	S and RBD	*Inhibition route and neutralizations* Tolerant to the N501Y RBD mutation Neutralization of the Alpha variant Effectively decrease viral burden after infections RBD-1-2G binding affinity to RBD-mFc (9.4 nM) and S1-hFc (6.9 nM) RBD-1-2G receptor-blocking capability (IC_{50} = 28.3 nM) High RBD binding affinity of RBD-1-2G (K_D = 14.3 nM), RBD-1-2G-Fc (K_D = 1.9 nM) and RBD-1-2G-Tri (K_D = 0.1 nM) *Inhibition of pseudo and live virus* Neutralization of pseudotyped viruses by RBD-1-2G (IC_{50} = 490 nM), RBD-1-2G-Fc (IC_{50} = 88 nM) and RBD-1-2G-Tri (IC_{50} = 4.1 nM) Neutralization of live virus by RBD-1-2G-Tri (IC_{50} = 182 nM) and RBD-1-2G-Fc (IC_{50} = 255 nM)	August 2022 [118]

Table 3 (Continued)

Nbs and Nb constructs	Source	SARS-CoV-2 target	Nbs for neutralization and therapeutics	Date and reference
aRBD-2-5-Fc–aRBD-2-7-Fc		–	Potent neutralization of authentic or pseudotyped viruses (wild-type and several strains) *Inhibition route* The aRBD-2-Fc bind variant RBDs (Alpha, Beta, Gamma, Delta, Delta plus, Omicron [BA.1 and BA.2], K_D = 1.20–7.96 nM) aRBD-2 recognizes an epitope close to the lateral loop of the RBM and partly overlaps the epitope of ACE2 Nbs bind the 'up' conformation aRBD-5 and aRBD-7 can also bind the 'down' conformation aRBD-5-Fc binds RBDs (wild-type, Alpha, Delta and Delta plus [K_D = 3.21–1.9 nM]) aRBD-5-Fc did not bind certain RBDs (Beta, Gamma, BA.1 and BA.2) aRBD-7-Fc only bound strongly to wild-type and Alpha RBDs (EC_{50} = 0.117 nM and 0.141 nM) *Inhibition of pseudo and live virus* aRBD-2-5-Fc (IC_{50} = 0.0511–0.1087 nM), and aRBD-2-7-Fc (IC_{50} = 0.0328–0.1914 nM) neutralized the Alpha and Gamma pseudotyped viruses High neutralization potency of aRBD-2-5-Fc and aRBD-2-7-Fc against wild-type, Beta, Delta and Omicron BA.1 variant live virus (IC_{50} = 0.0271–0.1299 nM) aRBD-2-5-Fc (IC_{50} = 0.0127–0.0311 nM) and aRBD-2-7-Fc (IC_{50} = 0.0319–0.0768 nM) neutralize Omicron BA.1, BA.1.1 and BA.2 aRBD-2-5-Fc and aRBD-2-7-Fc have higher activities than sotrovimab *Inhibition of in vivo infection* aRBD-2-5-Fc (10 mg/kg intraperitoneally) provided prophylactic protection against wild-type as well as prophylactic and therapeutic protection against the Omicron variant *in vivo* *Properties* aRBD-2-5-Fc is very stable *in vivo*	September 2022 [101]

SARS-CoV-2 severe acute respiratory syndrome coronavirus-2, *COVID-19* coronavirus disease 2019, *Nbs* nanobodies, *LOD* limit of detection, *RBD* receptor binding domain, *ACE2* angiotensin-converting enzyme 2, IC_{50} 50% inhibitory concentration, EC_{50} half maximal effective concentration, *Abs* antibodies, *ELISA* enzyme-linked immunosorbent assay, *RTC* replication transcription complex, *Ig* immunoglobulin, *hACE2* human ACE2, *STIP* short-term instantaneous prophylaxis, *SPR* surface plasmon resonance, *ITC* isothermal titration calorimetry, *sdAbs* single-domain antibodies, *RBM* receptor-binding motif, ND_{50} 50% neutralizing dose, ND_{90} 90% neutralizing dose, *Sbs* sybodies, *SA* South Africa, *IL* interleukin, *MERS-CoV* Middle East respiratory syndrome coronavirus, *HCoV* human coronavirus

Hamsters received nebulized exposure of normal saline with 25 mg/mL of NIH-CoVnb-112 for 20 min. After 24 h, hamsters were challenged with the SARS-CoV-2 prototype intranasally. Thereafter, more nebulization doses were administered at 12 h, 1 day and 2 days. In a COVID-19 hamster model, the administration of NIH-CoVnb-112 through nebulization resulted in a decrease in viral burden and lung pathology *in vivo* [96], which suggests the potential of NIH-CoVnb-112 as an inhalation treatment for SARS-CoV-2.

Six Nbs (7A3, 8A4, 1B5, 8A2, 2F7 and 1H6) that bind RBD and the S protein were isolated [97]. All V_HH-hFc showed binding affinity (nM) to the Wuhan-Hu-1 and B.1.1.7 variants. The 8A2, 7A3 and 1B5 (0.001–0.8 nM) Nbs demonstrated strong S binding for the B.1.351 and P.1 variants. Only 1B5 (0.14 nM) and 7A3 (0.42 nM) bound to B.1.617.2. The 7A3 and 1B5 Nbs bind to a similar epitope, while the other Nbs bind to a different epitope [97]. 1B5 (IC_{50} = 3.2 nM) and 8A2 (IC_{50} = 8 nM) were the best ACE2 blockers. 8A2 Nb showed potent ACE2 and pseudovirus inhibition [97] and was mostly a potent neutralizer of pseudovirus (IC_{50} = 5 nM) and virus with or without D614G. The 7A3 + 8A2 combination showed the highest neutralization efficacy against pseudovirus (IC_{50} = 0.2–1 nM), wild-type and variants (B.1.1.7, B.1.351, and P.1), and live virus (wild-type [IC_{50} = 20 nM]) and variants (D614G, B.1.1.7, B.1.351, P.1 and B.1.617.2 [IC_{50} 0.14–27 nM]) [97]. The 8A2 Nb hinders ACE2 binding to RBD in active conformation, whereas the 7A3 Nb binds the active and inactive conformation [97]. In the K18-hACE2 mouse model, 7A3 protects mice against B.1.351 and B.1.617.2, indicating its therapeutic potential against SARS-CoV-2 [97]. Moreover, 7A3 V_HH-hFc or 7A3+8A2 (5 mg/kg) protect K18-hACE2 mice against lethal B.1.351 infection; however, the protective efficiency of 7A3+8A2 (5 mg/kg) was decreased by 50% in K18-hACE2 mice exposed to a lethal dose of B.1.617.2.

Several studies investigated the effects of Nbs using *in vitro* neutralization assays (pseudo and live virus) and *in vivo* testing (Table 2). Comparing these studies, the Fc-MR17 Nb (K_D < 1 pM) showed the most potent binding affinity, followed by aRBD-2-5-Fc (K_D = 12.3 pM) and C5-Fc (K_D = 37 pM). The highest neutralization of pseudoviruses was by C5 (IC_{50} = 18–25 pM), followed by Nb_{15}-Fc, Nb_{22}-Fc, and Nb_{31}-Fc (IC_{50} = 10–28.8 pM). Interestingly, the highest live virus neutralization was by C5 trimer and C5-Fc (ND_{50} = 2–3 pM), followed by Nb_{15}-Fc, Nb_{22}-Fc, and Nb_{31}-Fc (IC_{50} = 41–75 pM). The *in vivo* concentration ranged from the lowest (20 µg,

NM1267 and NM1268, intranasal), middle/usual (5–10 mg/kg, intranasal) and highest (30 mg/kg, K874A, intranasal), which indicated prevention or treatment potential. Notably, C5-Fc, C5 trimer (intraperitoneal and/or intranasal) and Nb_{15}-Nb_H-Nb_{15} (intranasal) showed *in vivo* efficacy at 4–10 mg/mL.

Taken together, these studies clearly indicate the extremely positive contribution of Nbs in the discovery of efficient COVID-19 diagnosis methods and treatments (Table 3).

7 Conclusion

The devastating COVID-19 pandemic has greatly impacted the world both socially and economically. Current diagnosis and treatment options have been fairly effective, however there are various limitations/challenges associated with these options. Unfortunately, these challenges may negatively impact worldwide accessibility of COVID-19 diagnosis tests and treatments [5].

Notably, Nbs are an advantageous diagnostic and therapeutic option. The utilization of Nbs may overcome the challenges faced with current detection assays and medicines. Additionally, the potential aerosolization and inhalation delivery of Nbs allows for targeted treatment delivery as well as patient self-administration. Notably, Nbs can be rapidly and inexpensively generated, modified, tested (*in vitro* and *in vivo*), produced in large quantities, and developed into diagnosis tests as well as treatments. Although most SARS-CoV-2 Nbs have demonstrated high neutralization potency *in vitro*, further research is required to determine whether *in vitro* Nb potency is translated into *in vivo* and clinical therapeutic efficacy [5, 9]. Taken together, Nbs are proving to be a highly promising diagnosis and treatment option for COVID-19.

Acknowledgements The authors are grateful to the National Research foundation (120792 and 120820), SAMRC (JAF # 2020/127) and University of KwaZulu-Natal for financial support.

Declarations

Funding This research was funded by the National Research foundation (grant numbers 120792 and 120820), SAMRC (JAF # 2020/127), and University of KwaZulu-Natal.

Conflict of interest Dhaneshree Bestinee Naidoo and Anil Amichund Chuturgoon declare they have no conflicts of interest.

Ethics approval Not applicable.

Consent (participate and publication) Not applicable.

Author contributions Dhaneshree Bestinee Naidoo conceptualized and designed the review, searched the literature, and drafted and revised the manuscript. Anil Amichund Chuturgoon contributed to the conceptualization and critically revised the manuscript for important intellectual input. All authors have read and agreed to the published version of the manuscript.

Data availability statement Data sharing not applicable to this article as no datasets were generated or analysed.

Code availability Not applicable.

References

1. Badgujar KC, Badgujar VC, Badgujar SB. Vaccine development against coronavirus (2003 to present): an overview, recent advances, current scenario, opportunities and challenges. Diabetes Metab Syndr. 2020;14(5):1361–76.
2. Kirtipal N, Bharadwaj S, Kang SG. From SARS to SARS-CoV-2, insights on structure, pathogenicity and immunity aspects of pandemic human coronaviruses. Infect Genet Evol. 2020;85:104502.
3. Bchetnia M, et al. The outbreak of the novel severe acute respiratory syndrome coronavirus 2 (SARS-CoV-2): A review of the current global status. J Infect Public Health. 2020;13(11):1601–10.
4. Güttler T, et al. Neutralization of SARS-CoV-2 by highly potent, hyperthermostable, and mutation-tolerant nanobodies. EMBO J. 2021;40(19): e107985.
5. Nambulli S, et al. Inhalable nanobody (PiN-21) prevents and treats SARS-CoV-2 infections in Syrian hamsters at ultra-low doses. Sci Adv. 2021;7(22):eabh0319.
6. Konyak BM, et al. A systematic review on the emergence of omicron variant and recent advancement in therapies. Vaccines. 2022;10(9):1468.
7. Bessalah S, et al. Perspective on therapeutic and diagnostic potential of camel nanobodies for coronavirus disease-19 (COVID-19). 3 Biotech. 2021;11(2):89.
8. van Kasteren PB, et al. Comparison of seven commercial RT-PCR diagnostic kits for COVID-19. J Clin Virol. 2020;128:104412.
9. Stefan MA, et al. Development of potent and effective synthetic SARS-CoV-2 neutralizing nanobodies. MAbs. 2021;13(1):1958663.
10. Hoffmann M, et al. SARS-CoV-2 cell entry depends on ACE2 and TMPRSS2 and is blocked by a clinically proven protease inhibitor. Cell. 2020;181(2):271–80.
11. Schoof M, et al. An ultrapotent synthetic nanobody neutralizes SARS-CoV-2 by stabilizing inactive Spike. Science. 2020;370(6523):1473–9.
12. Koenig PA, et al. Structure-guided multivalent nanobodies block SARS-CoV-2 infection and suppress mutational escape. Science. 2021;371(6530):eabe6230.
13. Ren SY, et al. Omicron variant (B.1.1.529) of SARS-CoV-2: mutation, infectivity, transmission, and vaccine resistance. World J Clin Cases. 2022;10(1):1–11.
14. Zupancic JM, et al. Engineered multivalent nanobodies potently and broadly neutralize SARS-CoV-2 variants. Adv Ther (Weinh). 2021;4(8):2100099.
15. He X, et al. SARS-CoV-2 omicron variant: characteristics and prevention. MedComm (2020). 2021;2(4):838–45.
16. Zebardast A, et al. The role of single-domain antibodies (or nanobodies) in SARS-CoV-2 neutralization. Mol Biol Rep. 2022;49(1):647–56.

17. Pymm P, et al. Nanobody cocktails potently neutralize SARS-CoV-2 D614G N501Y variant and protect mice. Proc Natl Acad Sci USA. 2021;118(19): e2101918118.
18. Thakur S, et al. SARS-CoV-2 mutations and their impact on diagnostics, therapeutics and vaccines. Front Med. 2022;9: 815389.
19. Liang HY, et al. SARS-CoV-2 variants, current vaccines and therapeutic implications for COVID-19. Vaccines. 2022;10(9):1538.
20. Fernandes Q, et al. Emerging COVID-19 variants and their impact on SARS-CoV-2 diagnosis, therapeutics and vaccines. Ann Med. 2022;54(1):524–40.
21. Kannan S, et al. COVID-19 (novel coronavirus 2019)—recent trends. Eur Rev Med Pharmacol Sci. 2020;24(4):2006–11.
22. Girt GC, et al. The use of nanobodies in a sensitive ELISA test for SARS-CoV-2 Spike 1 protein. R Soc Open Sci. 2021;8(9): 211016.
23. Maniruzzaman M, et al. COVID-19 diagnostic methods in developing countries. Environ Sci Pollut Res Int. 2022;29(34):51384–97.
24. Alhamid G, et al. SARS-CoV-2 detection methods: a comprehensive review. Saudi J Biol Sci. 2022;29(11): 103465.
25. Ferré VM, et al. Omicron SARS-CoV-2 variant: what we know and what we don't. Anaesth Crit Care Pain Med. 2022;41(1): 100998.
26. Dhawan M, et al. Omicron variant (B.1.1.529) and its sublineages: what do we know so far amid the emergence of recombinant variants of SARS-CoV-2? Biomed Pharmacother. 2022;154:113522.
27. Mistry DA, et al. A systematic review of the sensitivity and specificity of lateral flow devices in the detection of SARS-CoV-2. BMC Infect Dis. 2021;21(1):828.
28. Bekliz M et al. Analytical sensitivity of eight different sARS-CoV-2 antigen-detecting rapid tests for omicron-BA.1 variant. Microbiol Spectr. 2022;10(4):e0085322.
29. Hardick J, et al. Evaluation of four point of care (POC) antigen assays for the detection of the SARS-CoV-2 variant omicron. Microbiol Spectr. 2022;10(3): e0102522.
30. Schrom J, et al. Comparison of SARS-CoV-2 reverse transcriptase polymerase chain reaction and BinaxNOW rapid antigen tests at a community site during an omicron surge: a cross-sectional study. Ann Intern Med. 2022;175(5):682–90.
31. Liang Y, et al. CRISPR-Cas12a-based detection for the major SARS-CoV-2 variants of concern. Microbiol Spectr. 2021;9(3): e0101721.
32. Liang Y, et al. Rapid detection and tracking of Omicron variant of SARS-CoV-2 using CRISPR-Cas12a-based assay. Biosens Bioelectron. 2022;205: 114098.
33. Liang Y, et al. Detection of major SARS-CoV-2 variants of concern in clinical samples via CRISPR-Cas12a-mediated mutation-specific assay. ACS Synth Biol. 2022;11(5):1811–23.
34. Wang Y, et al. Detection of SARS-CoV-2 and its mutated variants via CRISPR-Cas13-based transcription amplification. Anal Chem. 2021;93(7):3393–402.
35. Shanmugaraj B, et al. Perspectives on monoclonal antibody therapy as potential therapeutic intervention for coronavirus disease-19 (COVID-19). Asian Pac J Allergy Immunol. 2020;38(1):10–8.
36. Yousefi B, et al. A global treatments for coronaviruses including COVID-19. J Cell Physiol. 2020;235(12):9133–42.
37. Cao B, et al. A trial of lopinavir-ritonavir in adults hospitalized with severe covid-19. N Engl J Med. 2020;382(19):1787–99.
38. Şimşek-Yavuz S, Komsuoğlu Çelikyurt FI. An update of anti-viral treatment of COVID-19. Turk J Med Sci. 2021;51(SI-1):3372–90.
39. Qomara WF, et al. Effectiveness of remdesivir, lopinavir/ritonavir, and favipiravir for COVID-19 treatment: a systematic review. Int J Gen Med. 2021;14:8557–71.
40. Chen C, et al. Favipiravir versus arbidol for clinical recovery rate in moderate and severe adult COVID-19 patients: a prospective, multicenter, open-label, randomized controlled clinical trial. Front Pharmacol. 2021;12: 683296.
41. Wang M, et al. Remdesivir and chloroquine effectively inhibit the recently emerged novel coronavirus (2019-nCoV) in vitro. Cell Res. 2020;30(3):269–71.
42. Grein J, et al. Compassionate use of remdesivir for patients with severe covid-19. N Engl J Med. 2020;382(24):2327–36.
43. Axfors C, et al. Mortality outcomes with hydroxychloroquine and chloroquine in COVID-19 from an international collaborative meta-analysis of randomized trials. Nat Commun. 2021;12(1):2349.
44. Gao J, Hu S. Update on use of chloroquine/hydroxychloroquine to treat coronavirus disease 2019 (COVID-19). Biosci Trends. 2020;14(2):156–8.
45. Zhou H, et al. Sensitivity to vaccines, therapeutic antibodies, and viral entry inhibitors and advances to counter the SARS-CoV-2 omicron variant. Clin Microbiol Rev. 2022;35(3): e0001422.
46. Li P, et al. SARS-CoV-2 Omicron variant is highly sensitive to molnupiravir, nirmatrelvir, and the combination. Cell Res. 2022;32(3):322–4.
47. Lai CC, et al. The clinical efficacy and safety of anti-viral agents for non-hospitalized patients with COVID-19: a systematic review and network meta-analysis of randomized controlled trials. Viruses. 2022;14(8):1706.
48. Ye G, et al. The development of Nanosota-1 as anti-SARS-CoV-2 nanobody drug candidates. Elife. 2021;10: e64815.
49. Chen Z, et al. Humoral and cellular immune responses of COVID-19 vaccines against SARS-Cov-2 Omicron variant: a systemic review. Int J Biol Sci. 2022;18(12):4629–41.
50. Logunov DY, et al. Safety and immunogenicity of an rAd26 and rAd5 vector-based heterologous prime-boost COVID-19 vaccine in two formulations: two open, non-randomised phase 1/2 studies from Russia. Lancet. 2020;396(10255):887–97.
51. Jackson LA, et al. An mRNA vaccine against SARS-CoV-2—preliminary report. N Engl J Med. 2020;383(20):1920–31.
52. Wang Y, et al. Resistance of SARS-CoV-2 Omicron variant to convalescent and CoronaVac vaccine plasma. Emerg Microbes Infect. 2022;11(1):424–7.
53. Singhal T. The emergence of omicron: challenging times are here again! Indian J Pediatr. 2022;89(5):490–6.
54. Chenchula S, et al. Current evidence on efficacy of COVID-19 booster dose vaccination against the Omicron variant: a systematic review. J Med Virol. 2022;94(7):2969–76.
55. Gruell H, et al. mRNA booster immunization elicits potent neutralizing serum activity against the SARS-CoV-2 Omicron variant. Nat Med. 2022;28(3):477–80.
56. Muik A, et al. Neutralization of SARS-CoV-2 Omicron by BNT162b2 mRNA vaccine-elicited human sera. Science. 2022;375(6581):678–80.
57. He C, et al. A bivalent recombinant vaccine targeting the S1 protein induces neutralizing antibodies against both SARS-CoV-2 variants and wild-type of the virus. MedComm (2020). 2021;2(3):430–41.
58. World Health Organization. WHO recommends against the use of convalescent plasma to treat COVID-19. 2021. https://www.who.int/news/item/07-12-2021-who-recommends-against-the-use-of-convalescent-plasma-to-treat-covid-19.
59. Wu Y, et al. A noncompeting pair of human neutralizing antibodies block COVID-19 virus binding to its receptor ACE2. Science. 2020;368(6496):1274–8.
60. Shi R, et al. A human neutralizing antibody targets the receptor-binding site of SARS-CoV-2. Nature. 2020;584(7819):120–4.

61. Chi X, et al. A neutralizing human antibody binds to the N-terminal domain of the Spike protein of SARS-CoV-2. Science. 2020;369(6504):650–5.
62. Chen X, et al. Human monoclonal antibodies block the binding of SARS-CoV-2 spike protein to angiotensin converting enzyme 2 receptor. Cell Mol Immunol. 2020;17(6):647–9.
63. Ju B, et al. Human neutralizing antibodies elicited by SARS-CoV-2 infection. Nature. 2020;584(7819):115–9.
64. Pinto D, et al. Cross-neutralization of SARS-CoV-2 by a human monoclonal SARS-CoV antibody. Nature. 2020;583(7815):290–5.
65. Ma C, et al. Drastic decline in sera neutralization against SARS-CoV-2 Omicron variant in Wuhan COVID-19 convalescents. Emerg Microbes Infect. 2022;11(1):567–72.
66. Chen Z, et al. Potent monoclonal antibodies neutralize Omicron sublineages and other SARS-CoV-2 variants. Cell Rep. 2022;41(5): 111528.
67. Jiang S, Hillyer C, Du L. Neutralizing antibodies against SARS-CoV-2 and other human coronaviruses. Trends Immunol. 2020;41(5):355–9.
68. Tian X, et al. Potent binding of 2019 novel coronavirus spike protein by a SARS coronavirus-specific human monoclonal antibody. Emerg Microbes Infect. 2020;9(1):382–5.
69. Wang C, et al. A human monoclonal antibody blocking SARS-CoV-2 infection. Nat Commun. 2020;11(1):2251.
70. Starr TN, et al. Complete map of SARS-CoV-2 RBD mutations that escape the monoclonal antibody LY-CoV555 and its cocktail with LY-CoV016. Cell Rep Med. 2021;2(4): 100255.
71. Takashita E, et al. Efficacy of antibodies and antiviral drugs against Covid-19 omicron variant. N Engl J Med. 2022;386(10):995–8.
72. Naidoo DB, Chuturgoon AA. Nanobodies enhancing cancer visualization, diagnosis and therapeutics. Int J Mol Sci. 2021;22(18):9778.
73. Wang W, et al. Detection of SARS-CoV-2 in different types of clinical specimens. JAMA. 2020;323(18):1843–4.
74. Wu X, et al. A potent bispecific nanobody protects hACE2 mice against SARS-CoV-2 infection via intranasal administration. Cell Rep. 2021;37(3): 109869.
75. Wrapp D, et al. Structural basis for potent neutralization of betacoronaviruses by single-domain camelid antibodies. Cell. 2020;181(5):1004–15.
76. Chi X, et al. Humanized single domain antibodies neutralize SARS-CoV-2 by targeting the spike receptor binding domain. Nat Commun. 2020;11(1):4528.
77. Wagner TR, et al. NeutrobodyPlex-monitoring SARS-CoV-2 neutralizing immune responses using nanobodies. EMBO Rep. 2021;22(5): e52325.
78. Wagner TR, et al. Biparatopic nanobodies protect mice from lethal challenge with SARS-CoV-2 variants of concern. EMBO Rep. 2022;23(2): e53865.
79. Esposito G, et al. NMR-based analysis of nanobodies to SARS-CoV-2 Nsp9 reveals a possible antiviral strategy against COVID-19. Adv Biol (Weinh). 2021;5(12): e2101113.
80. Gransagne M, et al. Development of a highly specific and sensitive VHH-based sandwich immunoassay for the detection of the SARS-CoV-2 nucleoprotein. J Biol Chem. 2022;298(1): 101290.
81. Duarte JN, et al. Generation of immunity against pathogens via single-domain antibody-antigen constructs. J Immunol. 2016;197(12):4838–47.
82. Pishesha N, et al. A class II MHC-targeted vaccine elicits immunity against SARS-CoV-2 and its variants. Proc Natl Acad Sci USA. 2021;118(44): e2116147118.
83. Wu X, et al. Short-term instantaneous prophylaxis and efficient treatment against SARS-CoV-2 in hACE2 mice conferred by an intranasal nanobody (Nb22). Front Immunol. 2022;13: 865401.
84. Huo J, et al. Neutralizing nanobodies bind SARS-CoV-2 spike RBD and block interaction with ACE2. Nat Struct Mol Biol. 2020;27(9):846–54.
85. Dong J, et al. Development of multi-specific humanized llama antibodies blocking SARS-CoV-2/ACE2 interaction with high affinity and avidity. Emerg Microbes Infect. 2020;9(1):1034–6.
86. Hanke L, et al. An alpaca nanobody neutralizes SARS-CoV-2 by blocking receptor interaction. Nat Commun. 2020;11(1):4420.
87. Dong J, et al. Development of humanized tri-specifc nanobodies with potent neutralization for SARS-CoV-2. Sci Rep. 2020;10:17806.
88. Custódio TF, et al. Selection, biophysical and structural analysis of synthetic nanobodies that effectively neutralize SARS-CoV-2. Nat Commun. 2020;11(1):5588.
89. Xiang Y, et al. Versatile and multivalent nanobodies efficiently neutralize SARS-CoV-2. Science. 2020;370(6523):1479–84.
90. Li T, et al. A synthetic nanobody targeting RBD protects hamsters from SARS-CoV-2 infection. Nat Commun. 2022;13(1):4359.
91. Yao H, et al. A high-affinity RBD-targeting nanobody improves fusion partner's potency against SARS-CoV-2. PLoS Pathog. 2021;17(3): e1009328.
92. Gai J, et al. A potent neutralizing nanobody against SARS-CoV-2 with inhaled delivery potential. MedComm (2020). 2021;2(1):101–13.
93. Huo J, et al. A potent SARS-CoV-2 neutralising nanobody shows therapeutic efficacy in the Syrian golden hamster model of COVID-19. Nat Commun. 2021;12(1):5469.
94. Haga K, et al. Nasal delivery of single-domain antibody improves symptoms of SARS-CoV-2 infection in an animal model. PLoS Pathog. 2021;17(10): e1009542.
95. Esparza TJ, et al. High affinity nanobodies block SARS-CoV-2 spike receptor binding domain interaction with human angiotensin converting enzyme. Sci Rep. 2020;10(1):22370.
96. Esparza TJ, et al. Nebulized delivery of a broadly neutralizing SARS-CoV-2 RBD-specific nanobody prevents clinical, virological, and pathological disease in a Syrian hamster model of COVID-19. MAbs. 2022;14(1):2047144.
97. Hong J, et al. Dromedary camel nanobodies broadly neutralize SARS-CoV-2 variants. Proc Natl Acad Sci USA. 2022;119(18): e2201433119.
98. Li T, et al. A synthetic nanobody targeting RBD protects hamsters from SARS-CoV-2 infection. Nat Commun. 2021;12(1):4635.
99. Hanke L, et al. A bispecific monomeric nanobody induces spike trimer dimers and neutralizes SARS-CoV-2 in vivo. Nat Commun. 2022;13(1):155.
100. Titong A, et al. First-in-class trispecific VHH-Fc based antibody with potent prophylactic and therapeutic efficacy against SARS-CoV-2 and variants. Sci Rep. 2022;12(1):4163.
101. Ma H, et al. Hetero-bivalent nanobodies provide broad-spectrum protection against SARS-CoV-2 variants of concern including Omicron. Cell Res. 2022:1–12.
102. Anderson GP, et al. Single-domain antibodies for the detection of SARS-CoV-2 nucleocapsid protein. Anal Chem. 2021;93(19):7283–91.
103. Pagneux Q, et al. SARS-CoV-2 detection using a nanobody-functionalized voltammetric device. Commun Med (Lond). 2022;2:56.
104. Wu Y, et al. Identification of human single-domain antibodies against SARS-CoV-2. Cell Host Microbe. 2020;27(6):891–8.
105. Lu Q, et al. Development of multivalent nanobodies blocking SARS-CoV-2 infection by targeting RBD of spike protein. J Nanobiotechnology. 2021;19(1):33.
106. Valenzuela Nieto G, et al. Potent neutralization of clinical isolates of SARS-CoV-2 D614 and G614 variants by a monomeric, sub-nanomolar affinity nanobody. Sci Rep. 2021;11(1):3318.

107. Ma H, et al. Potent neutralization of SARS-CoV-2 by hetero-bivalent alpaca nanobodies targeting the spike receptor-binding domain. J Virol. 2021;95(10):e02438-e2520.
108. Xu J, et al. Nanobodies from camelid mice and llamas neutralize SARS-CoV-2 variants. Nature. 2021;595(7866):278–82.
109. Chen X, et al. A cell-free nanobody engineering platform rapidly generates SARS-CoV-2 neutralizing nanobodies. Nat Commun. 2021;12(1):5506.
110. Chi X, et al. An ultrapotent RBD-targeted biparatopic nanobody neutralizes broad SARS-CoV-2 variants. Signal Transduct Target Ther. 2022;7(1):44.
111. Ettich J, et al. A hybrid soluble gp130/spike-nanobody fusion protein simultaneously blocks interleukin-6 trans-signaling and cellular infection with SARS-CoV-2. J Virol. 2022;96(4): e0162221.
112. Favorskaya IA, et al. Single-domain antibodies efficiently neutralize SARS-CoV-2 variants of concern. Front Immunol. 2022;13: 822159.
113. Weinstein JB, et al. A potent alpaca-derived nanobody that neutralizes SARS-CoV-2 variants. iScience. 2022;25(3):103960.
114. Walter JD, et al. Biparatopic sybodies neutralize SARS-CoV-2 variants of concern and mitigate drug resistance. EMBO Rep. 2022;23(4): e54199.
115. Yang J, et al. A potent neutralizing nanobody targeting the spike receptor-binding domain of SARS-CoV-2 and the structural basis of its intimate binding. Front Immunol. 2022;13: 820336.
116. Li T, et al. Isolation, characterization, and structure-based engineering of a neutralizing nanobody against SARS-CoV-2. Int J Biol Macromol. 2022;209(Pt A):1379–88.
117. Li T, et al. Structural characterization of a neutralizing nanobody with broad activity against SARS-CoV-2 variants. Front Microbiol. 2022;13: 875840.
118. Fu Y, et al. A humanized nanobody phage display library yields potent binders of SARS CoV-2 spike. PLoS ONE. 2022;17(8): e0272364.